Reduced Order 4-D Var Data Assimilation

Ionel M. Navon, R. Ştefănescu

Department of Scientific Computing
Florida State University
Tallahassee, Florida

November 27, 2012

Contents

Contents

Contents

Contents

Contents

Contents

Contents

Contents

Contents

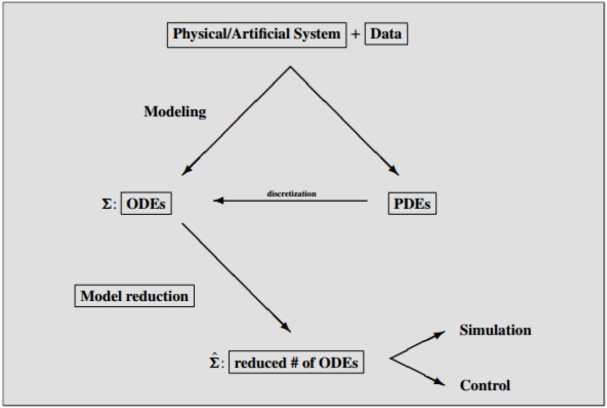

Fig.1 The broad setup

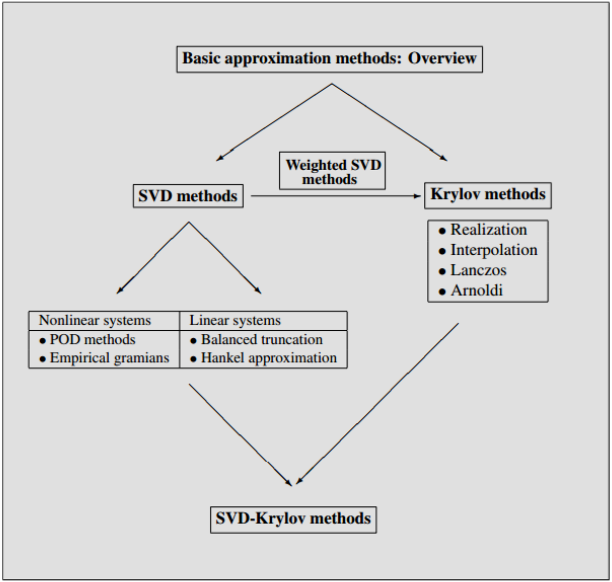

Fig.2 Flowchart of approximation methods and their interconnections

POD Galerkin reduced order model

- Let $y(x,t)$ with $x \in \Omega$ and $t \in (t_0, t_0 + T)$ be the state variable in the original system and let H be a Hilbert space.
- The complex flow, typically nonlinear and time dependent is governed by a system of PDE's.
- The PDE system comprised of an infinite numbers of degrees of freedom reads

$$\begin{cases} \text{Find } y(\cdot,t) \in \mathcal{H} \text{ satisfying :} \\ \dot{y}(x,t) = f(t, y(x,t)) \\ y(x,t_0) = y_0(x) \end{cases} \tag{1}$$

POD Galerkin reduced order model

- An approximation of (12) using well established numerical methods such as finite difference (FD) or finite element (FEM) with large number of degrees of freedom generates an ODE system that reads

$$\begin{cases} \text{Find } y(\cdot,t) \in \mathbb{R}^N \text{ satisfying :} \\ \dot{y}(x,t) = f(t, y(x,t)) \\ y(x,t_0) = y_0(x) \end{cases} \tag{2}$$

- The base premise of model reduction (MOR) is to approximate a full order model (2) using only a handful of degrees of freedom.
- The resulting low-dimensional model becomes a system of ODEs with a dramatically reduced dimension r ($r \ll N$)

POD Galerkin reduced order model

- POD is one of the most significant projection-based reduction methods for non-linear dynamical systems.
- It is also known as Karhunen - Loève expansion, principal component analysis in statistics, singular value decomposition (SVD) in matrix theory and empirical orthogonal functions (EOF) in meteorology and geophysical fluid dynamics
- Introduced in the field of turbulence by Lumley
- It was Sirovich (1987 a,b,c) that introduced the method of snapshots obtained from either experiments or numerical simulation

POD Galerkin reduced order model

- Generating POD-ROMs consists in first simulating the full-order system and then finding a set of "representative" state variable vectors (snapshots) to find an optimal basis $\{\varphi_1(x), .., \varphi_r(x)\}$
- Use of Galerkin projection to obtain a low-order dynamical system for the basis coefficients

$$\{a_1(t), a_2(t), ..., a_r(t)\}$$

POD Galerkin reduced-order model I

Algorithm

- Given $y(\cdot, t)$ from complex system 7 for $t \in (t_0, t_0 + T)$
  1. Compute a POD basis $\{\varphi_1(x), .., \varphi_r(x)\}$ such that

     $$X^r = span\{\varphi_1, \varphi_2, ..., \varphi_r\}$$

     is a good approximation to the data space

     $$\{y(\cdot, t)\}_{t \in (t_0, t_0+T)}$$

  2. Define reduced order approximation

     $$y_r(\cdot, t) = \sum_{j=1}^{r} \varphi_j(\cdot) a_j(t) \in X^r \tag{3}$$

     where $\{a_j(t)\}_{j=1}^{r}$ are the sought time varying POD basis coefficient functions.

POD Galerkin reduced-order model II

3. Substitute POD approximation into full-order system 7 and apply Galerkin procedure

$$\begin{cases} <\sum_{j=1}^{r}\varphi_j(\cdot)\dot{a}_j(t),\varphi_i(\cdot)>=<f(t,\sum_{j=1}^{r}\varphi_j(\cdot)a_j(t)),\varphi_i(\cdot)> \\ <\sum_{j=1}^{r}\varphi_j(\cdot)a_j(0),\varphi_i(\cdot)>=<y_0,\varphi_i(\cdot)>, \text{ for } i=1,..,r \end{cases}$$

yielding the POD-Galerkin ROM for $\{a_i(t)\}_{i=1}^{r}$

$$\begin{cases} \dot{a}_i(t)=<f(t,\sum_{j=1}^{r}\varphi_j(\cdot)a_j(t)),\varphi_i(\cdot)> \\ a_i(0)=<y_0,\varphi_i(\cdot)>, \text{ for } i=1,..,r \end{cases}$$

POD definition

- Assume $y(x,t) \in L^2(H, t_0, t_0+T)$ i.e.

$$\int_{t_0}^{t_0+T} |y(\cdot,t)|^2 dt < \infty$$

- Given time instances $t_1, t_2, .., t_M \in [0, T]$ consider ensemble of snapshots

$$S = span\{y(\cdot,t_1), ..., y(\cdot,t_M)\}$$

with $\mathrm{dim} S = M$.

- POD MOR methods seek a low dimensional (r) basis $\{\varphi_1, .., \varphi_r\}$ that optimally approximates the input collection s.t.

$$(*) \begin{cases} \min \dfrac{1}{M} \displaystyle\sum_{l=1}^{M} \| y(\cdot,t_l) - \sum_{j=1}^{r} < y(\cdot,t_l), \varphi_j(\cdot) >_H \varphi_j(\cdot) \|_H^2 \\ \quad \text{s.t. conditions that} \\ < \varphi_i, \varphi_j >_H = \delta_{i,j}, \quad 1 \le i,j \le r \le M \\ \quad \delta_{i,j} \text{ is the Kroneker delta.} \end{cases}$$

POD definition

- To solve it we consider the eigenvalue problem

  $$Kv = \lambda v, \;\; K \in \mathbb{R}^{M \times M}$$

  and

  $$K_{kl} = \frac{1}{M} < y(\cdot, t_l), y(\cdot, t_k) >_H$$

  is the snapshot correlation matrix, $v_j, \; j = 1, .., M$ are the eigenvectors

  $$\lambda_M \leq ... \leq \lambda_2 \leq \lambda_1$$

  are the positive eigenvalues.

- Then solution of (*) is given by

  $$\varphi_j(\cdot) = \frac{1}{\sqrt{\lambda_j}} \sum_{l=1}^{M} (v_j)_l y(\cdot, t_l), \;\; 1 \leq j \;\; \leq r$$

  where $(v_j)_l$ is the $l-$th component of the eigenvector v_j.

I.M. Navon, R. Ştefănescu

POD definition

- A known error estimate is

$$\frac{1}{M}\sum_{l=1}^{M}||y(\cdot,t_l)-\sum_{j=1}^{r}< y(\cdot,t_l),\varphi_j(\cdot) >_H \varphi_j(\cdot)||_H^2=\sum_{j=r+1}^{M}\lambda_j.$$

- The relative error in L_2

$$\varepsilon=\frac{\frac{1}{T}\int_{t_0}^{t_0+T}||y(\cdot,t)-\sum_{j=1}^{r}< y(\cdot,t),\varphi_j(\cdot) >_H \varphi_j(\cdot)||_2^2dt}{\frac{1}{T}\int_{t_0}^{t_0+T}||y(\cdot,t)||_2^2dt}=\frac{\sum_{j=r+1}^{M}\lambda_j}{\sum_{j=1}^{M}\lambda_j}.$$

- ε is a heuristic criterion to determine number of POD modes to be retained in the ROM

POD/DEIM POD/EIM justification and methodology

- Model order reduction : Reduce the computational complexity/time of large scale dynamical systems by approximations of much lower dimension with nearly the same input/output response characteristics.

- Goal : Construct reduced-order model for different types of discretization method (finite difference (FD), finite element (FEM), finite volume (FV)) of unsteady and/or parametrized nonlinear PDEs. E.g., PDE:

$$\frac{\partial y}{\partial t}(x,t) = \mathrm{L}(y(x,t)) + \mathrm{F}(y(x,t)),\ \ t \in [0,T]$$

where L is a linear function and F a nonlinear one.

POD/DEIM methodology applied to FD SCHEMES

- The corresponding FD scheme is a n dimensional ordinary differential system

$$\frac{d}{dt}\mathbf{y}(t) = A\mathbf{y}(t) + \mathbf{F}(\mathbf{y}(t)),\ A \in \mathbb{R}^{n\times n},$$

where $\mathbf{y}(t) = [y_1(t), y_2(t), .., y_n(t)] \in \mathbb{R}^n$ and $y_i(t) \in \mathbb{R}$ are the spatial components $y(x_i, t),\ i = 1, .., n$. $\mathbf{F}$ is a nonlinear function evaluated at $\mathbf{y}(t)$ componentwise, i.e. $\mathbf{F} = [\mathrm{F}(y_1(t)), .., \mathrm{F}(y_n(t))]^T$, $\mathrm{F} : I \subset \mathbb{R} \to \mathbb{R}$.

POD/DEIM methodology applied to FD SCHEMES

- A common model order reduction method involves the Galerkin projection with basis $V_k \in \mathbb{R}^{n\times k}$ obtained from Proper Orthogonal Decomposition (POD), for $k \ll n$, i.e. $\mathbf{y} \approx V_k\tilde{\mathbf{y}}(\mathbf{t})$, $\tilde{\mathbf{y}}(\mathbf{t}) \in \mathbb{R}^k$. Applying an inner product to the ODE discrete system we get

$$\frac{d}{dt}\tilde{\mathbf{y}}(\mathbf{t}) = \underbrace{V_k^T A V_k}_{k\times k}\tilde{\mathbf{y}}(\mathbf{t}) + \underbrace{V_k^T \mathbf{F}(V_k\tilde{\mathbf{y}}(\mathbf{t}))}_{\tilde{N}(\tilde{\mathbf{y}})} \tag{4}$$

POD/DEIM methodology applied to FD SCHEMES

- The efficiency of POD - Galerkin technique is limited to the linear or bilinear terms. The projected nonlinear term still depends on the dimension of the original system

$$\tilde{N}(\tilde{\mathbf{y}}) = \underbrace{V_k^T}_{k\times n} \underbrace{\mathbf{F}(V_k\tilde{\mathbf{y}}(\mathbf{t}))}_{n\times 1}.$$

- To mitigate this inefficiency we introduce "Discrete Empirical Interpolation Method (DEIM) " for nonlinear approximation. For $m \ll n$

$$\tilde{N}(\tilde{\mathbf{y}}) \approx \underbrace{V_k^T U(P^T U)^{-1}}_{precomputed \;\; k\times m} \underbrace{\mathbf{F}(P^T V_k\tilde{\mathbf{y}}(\mathbf{t}))}_{m\times 1}.$$

POD/EIM methodology applied to FE SCHEMES

- The corresponding Finite Element (FE) scheme is a n dimensional ordinary differential system

$$\mathbf{M}_h \frac{d}{dt}\mathbf{y}(t) = \mathbf{K}_h\mathbf{y}(t) + \mathbf{N}_h(\mathbf{y}(t)),\ \ \mathbf{M}_h, \mathbf{K}_h \in \mathbb{R}^{n\times n}, \tag{5}$$

- $\mathbf{M}_h$ is the mass matrix
- $\mathbf{K}_h$ corresponds to the linear terms in the PDE

$$\mathbf{y}(t) = [y_1(t), y_2(t), .., y_n(t)] \in \mathbb{R}^n,\ \ y_i(t) \in \mathbb{R}.$$

$$y(t,x) \simeq \sum_{j=1}^{n} \psi_j(x) y_j(t) = \Psi(x)\mathbf{y}(t),\ \ \Psi(x) \in \mathbb{R}^{1\times n}.$$

POD/EIM methodology applied to FE SCHEMES

- $\mathbf{N}_h(\mathbf{y}(t)) \in \mathbb{R}^n$ is a nonlinear functional which can be of the following form

$$[\mathbf{N}_h(\mathbf{y}(t))]_i = \int_\Omega \frac{\partial \psi_i(x)}{\partial x} F(\Psi(x)\mathbf{y}(t)) d\Omega, \;\; i = 1, ..n.$$

$$[\mathbf{N}_h(\mathbf{y}(t))]_i = \int_\Omega \psi_i(x) F(\Psi(x)\mathbf{y}(t)) d\Omega, \;\; i = 1, ..n.$$

POD/EIM methodology applied to FE SCHEMES

- Using the Galerkin projection with basis $\Phi(x) = \Psi(x) U_k$, $\Phi(x) \in \mathbb{R}^{1\times k}$, $U_k \in \mathbb{R}^{n\times k}$ calculated via POD, for $k \ll n$, i.e. $y(t,x) \approx \Phi(x)\tilde{\mathbf{y}}(\mathbf{t})$, $\tilde{\mathbf{y}}(\mathbf{t}) \in \mathbb{R}^k$ we apply the following inner product

$$< x, y >_{\mathbf{M}_h} = x^T \mathbf{M}_h y.$$

One obtains the corresponding discretized reduced order model:

$$\underbrace{U_k^T \mathbf{M}_h U_k}_{\mathbf{I}\in\mathbb{R}^{\mathbf{k}\times\mathbf{k}}} \frac{d}{dt}\tilde{\mathbf{y}}(\mathbf{t}) = \underbrace{U_k^T \mathbf{K}_h U_k}_{k\times k} \tilde{\mathbf{y}}(\mathbf{t}) + \underbrace{U_k^T \mathbf{N_h}(\tilde{\mathbf{y}}(\mathbf{t}))}_{\tilde{\mathbf{N}}(\tilde{\mathbf{y}}(\mathbf{t}))}. \tag{6}$$

POD/EIM methodology applied to FE SCHEMES

- The projected nonlinear term still depends on the dimension of the original system

$$\tilde{N}(\tilde{\mathbf{y}}(\mathbf{t})) = \underbrace{U_k^T}_{k\times n} \underbrace{\mathbf{N_h}(\tilde{\mathbf{y}}(\mathbf{t}))}_{n\times 1}.$$

$$[\mathbf{N}_h(\tilde{\mathbf{y}}(\mathbf{t}))]_i = \int_\Omega \psi_i(x) F(\Phi(x)\tilde{\mathbf{y}}(\mathbf{t})) d\Omega, \;\; i = 1, ..n.$$

POD/EIM methodology applied to FE SCHEMES

- The Empirical Interpolation Method (EIM) approximation of the nonlinear function $F(\Phi(x)\tilde{\mathbf{y}}(\mathbf{t}))$ is given by

$$F(\Phi(x)\tilde{\mathbf{y}}(\mathbf{t})) \simeq \mathbf{Q}(x)\rho(t) = \mathbf{Q}(x)(\mathbf{Q}(\mathbf{z}))^{-1}F(\Phi(\mathbf{z})\tilde{\mathbf{y}}(\mathbf{t})),$$

$$\mathbf{Q}(x) = [q_1(x), ..., q_m(x)],\ \mathbf{z} = [z_1, ..., z_m],\ m \ll n$$
$$\mathbf{Q}(\mathbf{z}) \in \mathbb{R}^{m\times m},\ \Phi(\mathbf{z}) \in \mathbb{R}^{m\times k},$$
$$F(\Phi(\mathbf{z})\tilde{\mathbf{y}}(\mathbf{t})) \in \mathbb{R}^{m\times 1} - F \text{ is applied componentwise}$$

POD/EIM methodology applied to FE SCHEMES

- Thus

$$\mathbf{N}_h(\tilde{\mathbf{y}}(\mathbf{t})) \simeq \underbrace{\int_\Omega \Psi(x)^T Q(x) d\Omega}_{n\times m} \underbrace{(\mathbf{Q}(\mathbf{z}))^{-1}}_{m\times m} \underbrace{F(\Phi(\mathbf{z})\tilde{\mathbf{y}}(\mathbf{t}))}_{m\times 1}$$

- Now we are able to separate the unknown $\tilde{\mathbf{y}}(\mathbf{t})$ from the integrals allowing us the precomputation of the integrals which then can be used in all of the time steps.

$$\tilde{N}(\tilde{\mathbf{y}}(\mathbf{t})) \simeq \underbrace{U_k^T}_{k\times n} \underbrace{\int_\Omega \Psi(x)^T Q(x) d\Omega (\mathbf{Q}(\mathbf{z}))^{-1}}_{n\times m} \underbrace{F(\Phi(\mathbf{z})\tilde{\mathbf{y}}(\mathbf{t}))}_{m\times 1}.$$

POD/DEIM nonlinear model reduction for SWE

- We applied DEIM to a POD alternating direction implicit (ADI) FD scheme of the SWE on a rectangular domain.
- We considered the alternating direction fully implicit finite-difference scheme (Gustafsson 1971, Fairweather and Navon 1980, Navon and De Villiers 1986, Kreiss and Widlund 1966) on a rectangular domain since the scheme remains stable at large Courant numbers (CFL).

SWE model

$$\frac{\partial w}{\partial t} = A(w)\frac{\partial w}{\partial x} + B(w)\frac{\partial w}{\partial y} + C(y)w, \tag{7}$$

$$0 \le x \le L,\ 0 \le y \le D,\ \ t \in [0, t_f],$$

where $w = (u, v, \phi)^T$, u, v are the velocity components in the x and y directions, respectively, h is the depth of the fluid, g is the acceleration due to gravity and $\phi = 2\sqrt{gh}$.
The matrices A, B and C are expressed

$$A = -\begin{pmatrix} u & 0 & \phi/2 \\ 0 & u & 0 \\ \phi/2 & 0 & u \end{pmatrix},\ B = -\begin{pmatrix} v & 0 & 0 \\ 0 & v & \phi/2 \\ 0 & \phi/2 & v \end{pmatrix}$$

$$C = \begin{pmatrix} 0 & f & 0 \\ -f & 0 & 0 \\ 0 & 0 & 0 \end{pmatrix},$$

$f = \hat{f} + \beta(y - D/2)$ (Coriolis force), $\beta = \dfrac{\partial f}{\partial y}$, with $\hat{f}$ and β constants.

I.M. Navon, R. Ştefănescu

SWE model

- We assume periodic solutions in the x-direction

$$w(x, y, t) = w(x + L, y, t),$$

while in the $y-$direction we have

$$v(x, 0, t) = v(x, D, t) = 0.$$

- The initial conditions are derived from the initial height-field condition No. 1 of Grammelvedt (1969), i.e.

$$h(x, y) = H_0 + H_1 + \tanh\left(9\frac{D/2 - y}{2D}\right) + H_2 \operatorname{sech}^2\left(9\frac{D/2 - y}{2D}\right)\sin\left(\frac{2\pi x}{L}\right)$$

I.M. Navon, R. Ştefănescu

POD History

POD Galerkin reduced order model

POD definition

POD/DEIM POD/EIM justification and methodology

POD/DEIM nonlinear model reduction for SWE

POD/DEIM as a discrete variant of EIM and their pseudo - algorithms

Dual weighted POD in 4-D Var data assimilation

Proper orthogonal decomposition of structurally dominated turbulent flows

Trust Region POD 4-D VAR of the limited area FEM SWE

SWE model

- The initial velocity fields were derived from the initial height field using the geostrophic relationship

$$u = \left(\frac{-g}{f}\right)\frac{\partial h}{\partial y}, \;\; v = \left(\frac{g}{f}\right)\frac{\partial h}{\partial x}.$$

- The constants used were:

$$\begin{aligned} L &= 6000km & g &= 10ms^{-2} \\ D &= 4400km & H_0 &= 2000m \\ \hat{f} &= 10^{-4}s^{-1} & H_1 &= 220mm \\ \beta &= 1.5\cdot 10^{-11}s^{-1}m^{-1} & H_2 &= 133m. \end{aligned}$$

The nonlinear Gustafsson ADI finite difference implicit scheme

- First we introduce a network of $N_x \cdot N_y$ equidistant points on $[0, L] \times [0, D]$, with $dx = L/(N_x - 1)$, $dy = D/(N_y - 1)$. We also discretize the time interval $[0, t_f]$ using NT equally distributed points and $dt = t_f/(NT - 1)$.

- Next we define vectors of unknown variables of dimension $n_{xy} = N_x \cdot N_y$ containing approximate solutions such as

$$\mathbf{u}(t) \approx u(x_i, y_j, t), \mathbf{v}(t) \approx v(x_i, y_j, t), \boldsymbol{\phi} \approx \phi(x_i, y_j, t) \in \mathbb{R}^{n_{xy}}$$

- The idea behind the ADI method is to split the finite difference equations into two, one with the x-derivative taken implicitly and the next with the y-derivative taken implicitly,

- For t_{n+1}, the Gustafsson nonlinear ADI difference scheme is defined by

  I. First step - get solution at $t(n+\frac{1}{2})$

$$
\begin{aligned}
&\mathbf{u}(t_{n+\frac{1}{2}}) + \frac{\Delta t}{2} F_{11}\Big(\mathbf{u}(t_{n+\frac{1}{2}}), \phi(t_{n+\frac{1}{2}})\Big) = \mathbf{u}(t_n) - \frac{\Delta t}{2} F_{12}\Big(\mathbf{u}(t_n), \mathbf{v}(t_n)\Big) + \\
&\qquad \frac{\Delta t}{2} [\underbrace{f, f, .., f}_{N_x}]^T * \mathbf{v}(t_n), \\
&\mathbf{v}(t_{n+\frac{1}{2}}) + \frac{\Delta t}{2} F_{21}\Big(\mathbf{u}(t_{n+\frac{1}{2}}), \mathbf{v}(t_{n+\frac{1}{2}})\Big) + \frac{\Delta t}{2} [\underbrace{f, f, .., f}_{N_x}]^T * \mathbf{u}(t_{n+\frac{1}{2}}) = \mathbf{v}(t_n) - \\
&\qquad \frac{\Delta t}{2} F_{22}\Big(\mathbf{v}(t_n), \phi(t_n)\Big), \\
&\phi(t_{n+\frac{1}{2}}) + \frac{\Delta t}{2} F_{31}\Big(\mathbf{u}(t_{n+\frac{1}{2}}), \phi(t_{n+\frac{1}{2}})\Big) = \phi(t_n) - \frac{\Delta t}{2} F_{32}\Big(\mathbf{v}(t_n), \phi(t_n)\Big),
\end{aligned}
\tag{8}
$$

  with "*" denoting MATLAB componentwise multiplication and the nonlinear functions $F_{11}, F_{12}, F_{21}, F_{22}, F_{31}, F_{32} : \mathbb{R}^{n_{xy}} \times \mathbb{R}^{n_{xy}} \to \mathbb{R}^{n_{xy}}$ are defined as follows

The nonlinear Gustafsson ADI finite difference implicit scheme

$$F_{11}(\mathbf{u},\phi) = \mathbf{u} * A_x\mathbf{u} + \frac{1}{2}\phi * A_x\phi,$$

$$F_{12}(\mathbf{u},\mathbf{v}) = \mathbf{v} * A_y\mathbf{u},\, F_{21}(\mathbf{u},\mathbf{v}) = \mathbf{u} * A_x\mathbf{v},$$

$$F_{22}(\mathbf{v},\phi) = \mathbf{v} * A_y\mathbf{v} + \frac{1}{2}\phi * A_y\phi,$$

$$F_{31}(\mathbf{u},\phi) = \frac{1}{2}\phi * A_x\mathbf{u} + \mathbf{u} * A_x\phi,$$

$$F_{32}(\mathbf{v},\phi) = \frac{1}{2}\phi * A_y\mathbf{v} + \mathbf{v} * A_y\phi,$$

where $A_x, A_y \in \mathbb{R}^{n_{xy}\times n_{xy}}$ are constant coefficient matrices for discrete first-order and second-order differential operators which take into account the boundary conditions.

The Quasi-Newton Method

- The nonlinear systems of algebraic equations denoted by $g(\alpha) = 0$ are solved using the quasi-Newton method.
- The computationally expensive LU decomposition is performed only once every $M - th$ time-step, where M is a fixed integer.
- The quasi-Newton formula is

$$\alpha^{(m+1)} = \alpha^{(m)} - \hat{J}^{-1}(\alpha^{(m)})g(\alpha^{(m)}), \text{ where}$$

$$\hat{J} = J(\alpha^{(0)}) + O(dt).$$

The POD version of SWE model

- The POD reduced-order system is constructed by applying the Galerkin projection method to ADI FD discrete model by first replacing $\mathbf{u}, \mathbf{v}, \phi$ with their POD based approximation $U\tilde{u}$, $V\tilde{v}$, $\Phi\tilde{\phi}$, respectively, and then premultiplying the corresponding equations by U^T, V^T and Φ^T, the POD bases.

- The resulting POD reduced system for the first step $(t_{n+\frac{1}{2}})$ of the ADI FD scheme is

$$
\begin{aligned}
\tilde{u}(t_{n+\frac{1}{2}}) + \frac{\Delta t}{2} U^T \tilde{F}_{11}\Big(\tilde{u}(t_{n+\frac{1}{2}}), \tilde{\phi}(t_{n+\frac{1}{2}})\Big) &= \tilde{u}(t_n) - \frac{\Delta t}{2} U^T \tilde{F}_{12}\Big(\tilde{u}(t_n), \tilde{v}(t_n)\Big) \\
&\quad + \frac{\Delta t}{2} U^T \Big(\underbrace{[f, f, .., f]}_{N_x}{}^T * V\tilde{v}(t_n)\Big), \\
\tilde{v}(t_{n+\frac{1}{2}}) + \frac{\Delta t}{2} V^T \tilde{F}_{21}\Big(\tilde{u}(t_{n+\frac{1}{2}}), \tilde{v}(t_{n+\frac{1}{2}})\Big) + \frac{\Delta t}{2} V^T \Big(\underbrace{[f, f, .., f]}_{N_x}{}^T * U\tilde{u}(t_{n+\frac{1}{2}})\Big) \\
&= \tilde{v}(t_n) - \frac{\Delta t}{2} V^T \tilde{F}_{22}\Big(\tilde{v}(t_n), \tilde{\phi}(t_n)\Big), \\
\tilde{\phi}(t_{n+\frac{1}{2}}) + \frac{\Delta t}{2} \Phi^T \tilde{F}_{31}\Big(\tilde{u}(t_{n+\frac{1}{2}}), \tilde{\phi}(t_{n+\frac{1}{2}})\Big) &= \tilde{\phi}(t_n) - \frac{\Delta t}{2} \Phi^T \tilde{F}_{32}\Big(\tilde{v}(t_n), \tilde{\phi}(t_n)\Big),
\end{aligned}
\tag{9}
$$

where $\tilde{F}_{11}, \tilde{F}_{12}, \tilde{F}_{21}, \tilde{F}_{22}, \tilde{F}_{31}, \tilde{F}_{32} : \mathbb{R}^k \times \mathbb{R}^k \to \mathbb{R}^k$ are defined by

The POD version of SWE model

$$
\begin{aligned}
\tilde{F}_{11}(\tilde{u},\tilde{\phi}) &= (U\tilde{u}) * (\underbrace{A_x U}\,\tilde{u}) + \frac{1}{2}(\Phi\tilde{\phi}) * (\underbrace{A_x \Phi}\,\tilde{\phi}),\\
\tilde{F}_{12}(\tilde{u},\tilde{v}) &= (V\tilde{v}) * (\underbrace{A_y U}\,\tilde{u}),\ \tilde{F}_{21}(\tilde{u},\tilde{v}) = (U\tilde{u}) * (\underbrace{A_x V}\,\tilde{v}),\\
\tilde{F}_{22}(\tilde{v},\tilde{\phi}) &= (V\tilde{v}) * (\underbrace{A_y V}\,\tilde{v}) + \frac{1}{2}(\Phi\tilde{\phi}) * (\underbrace{A_y \Phi}\,\tilde{\phi}),\\
\tilde{F}_{31}(\tilde{u},\tilde{\phi}) &= \frac{1}{2}(\Phi\tilde{\phi}) * (\underbrace{A_x U}\,\tilde{u}) + (U\tilde{u}) * (\underbrace{A_x \Phi}\,\tilde{\phi}),\\
\tilde{F}_{32}(\tilde{v},\tilde{\phi}) &= \frac{1}{2}(\Phi\tilde{\phi}) * (\underbrace{A_y V}\,\tilde{v}) + (V\tilde{v}) * (\underbrace{A_y \Phi}\,\tilde{\phi}).
\end{aligned}
\tag{10}
$$

The POD version of SWE model

- The coefficient matrices defined in the linear terms of the POD reduced system as well as the coefficient matrices in the nonlinear functions (i.e. $A_x U, A_y U,$ $A_x V, A_y V, A_x \Phi, A_y \Phi \in \mathbb{R}^{n\times k}$ grouped by the curly braces) can be precomputed, saved and re-used in all time steps.
- However, performing the componentwise multiplications in (10) and computing the projected nonlinear terms in (9)

$$\begin{aligned}&\underbrace{U^T}_{k\times n_{xy}}\underbrace{\tilde{F}_{11}(\tilde{u},\tilde{\phi})}_{n_{xy}\times 1}, U^T\tilde{F}_{12}(\tilde{u},\tilde{v}), V^T\tilde{F}_{21}(\tilde{u},\tilde{v}),\\ &V^T\tilde{F}_{22}(\tilde{v},\tilde{\phi}), \Phi^T\tilde{F}_{31}(\tilde{u},\tilde{\phi}), \Phi^T\tilde{F}_{32}(\tilde{v},\tilde{\phi}),\end{aligned} \tag{11}$$

still have computational complexities depending on the dimension n_{xy} of the original system from both evaluating the nonlinear functions and performing matrix multiplications to project on POD bases.

Discrete Empirical Interpolation Method (DEIM)

- DEIM is a discrete variation of the Empirical Interpolation method proposed by Barrault et al. (2004). The application was suggested by Chaturantabut and Sorensen (2008, 2010, 2012).
- Let $f : D \to \mathbb{R}^n,\ D \subset \mathbb{R}^n$ be a nonlinear function. If $U = \{u_l\}_{l=1}^m,\ u_i \in \mathbb{R}^n,\ i = 1, .., m$ is a linearly independent set, for $m \leq n$, then for $\tau \in D$, the DEIM approximation of order m for $f(\tau)$ in the space spanned by $\{u_l\}_{l=1}^m$ is given by

$$f(\tau) \approx Uc(\tau),\ U \in \mathbb{R}^{n \times m},\ c(\tau) \in \mathbb{R}^m. \tag{12}$$

- The basis U can be constructed effectively by applying the POD method on the nonlinear snapshots $f(\tau^{t_i}),\ i = 1, .., n_s$.

Discrete Empirical Interpolation Method (DEIM)

- Interpolation is used to determine the coefficient vector $c(\tau)$ by selecting m rows $\rho_1, .., \rho_m,\ \rho_i \in \mathbb{N}^*$, of the overdetermined linear system (12)

$$\underbrace{\begin{bmatrix} f_1(\tau) \\ \vdots \\ \vdots \\ f_n(\tau) \end{bmatrix}}_{f(\tau)\in\mathbb{R}^n} = \underbrace{\begin{bmatrix} u_{11} & \dots & u_{1m} \\ \vdots & \dots & \vdots \\ \vdots & \dots & \vdots \\ u_{n1} & \dots & u_{nm} \end{bmatrix}}_{U\in\mathbb{R}^{n\times m}} \underbrace{\begin{bmatrix} c_1(\tau) \\ \vdots \\ c_m(\tau) \end{bmatrix}}_{c(\tau)\in\mathbb{R}^m}.$$

to form a m-by-m linear system

$$\underbrace{\begin{bmatrix} f_{\rho_1}(\tau) \\ \vdots \\ f_{\rho_m}(\tau) \end{bmatrix}}_{f_{\vec{\rho}}(\tau)\in\mathbb{R}^m} = \underbrace{\begin{bmatrix} u_{\rho_1 1} & \dots & u_{\rho_1 m} \\ \vdots & \dots & \vdots \\ u_{\rho_m 1} & \dots & u_{\rho_m m} \end{bmatrix}}_{U_{\vec{\rho}}\in\mathbb{R}^{m\times m}} \underbrace{\begin{bmatrix} c_1(\tau) \\ \vdots \\ c_m(\tau) \end{bmatrix}}_{c(\tau)\in\mathbb{R}^m}.$$

I.M. Navon, R. Ştefănescu

Discrete Empirical Interpolation Method (DEIM)

- In the short notation form

$$U_{\vec{\rho}} c(\tau) = f_{\vec{\rho}}(\tau).$$

- Lemma 2.3.1 in Chaturantabut (2008) proves that $U_{\vec{\rho}}$ is invertible, thus we can uniquely determine $c(\tau)$

$$c(\tau) = U_{\vec{\rho}}^{-1} f_{\vec{\rho}}(\tau).$$

- The DEIM approximation of $F(\tau) \in \mathbb{R}^n$ is

$$f(\tau) \approx Uc(\tau) = UU_{\vec{\rho}}^{-1} f_{\vec{\rho}}(\tau).$$

Discrete Empirical Interpolation Method (DEIM)

- $U_{\vec{\rho}}$ and $f_{\vec{\rho}}(\tau)$ can be written in terms of U and $f(\tau)$

$$U_{\vec{\rho}} = P^T U, \qquad f_{\vec{\rho}}(\tau) = P^T f(\tau)$$

where

$$P = [e_{\rho_1}, .., e_{\rho_m}] \in \mathbb{R}^{n \times m}, \;\; e_{\rho_i} = [0, ..0, \underbrace{1}_{\rho_i}, 0, .., 0]^T \in \mathbb{R}^n.$$

- The DEIM approximation of $f \in \mathbb{R}^n$ becomes

$$f(\tau) \approx U(P^T U)^{-1} P^T f(\tau).$$

Discrete Empirical Interpolation Method (DEIM)

- Using the DEIM approximation, the complexity for computing the nonlinear term of the reduced system in each time step is now independent of the dimension n of the original full-order sytem.
- The only unknowns need to be specified are the indices $\rho_1, \rho_2, ..., \rho_m$ or matrix P.

DEIM: Algorithm for Interpolation Indices

INPUT: $\{u_l\}_{l=1}^{m} \subset \mathbb{R}^n$ (linearly independent):

OUTPUT: $\vec{\rho} = [\rho_1, .., \rho_m] \in \mathbb{R}^m$

1. $[|\psi| \quad \rho_1] = max|u_1|, \psi \in \mathbb{R}$ and ρ_1 is the component position of the largest absolute value of u_1, with the smallest index taken in case of a tie.
2. $U = [u_1],\ P = [e_{\rho_1}],\ \vec{\rho} = [\rho_1]$.
3. For $l = 2, .., m$ do
   - **a** Solve $(P^T U)c = P^T u_l$ for c
   - **b** $r = u_l - Uc$
   - **c** $[|\psi| \quad \rho_l] = max\{|r|\}$
   - **d** $U \leftarrow [U \quad u_l],\ P \leftarrow [P \quad e_{\rho_l}],\ \vec{\rho} \leftarrow \begin{bmatrix} \vec{\rho} \\ \rho_l \end{bmatrix}$
4. end for.

The DEIM version of SWE model

- DEIM is used to remove this dependency.
- The projected nonlinear functions can be approximated by DEIM in a form that enables precomputation so that the computational cost is decreased and independent of the original system.
- Only a few entries of the nonlinear term corresponding to the specially selected interpolation indices from DEIM must be evaluated at each time step.
- DEIM approximation is applied to each of the nonlinear functions $\tilde{F}_{11}, \tilde{F}_{12}, \tilde{F}_{21}, \tilde{F}_{22}, \tilde{F}_{31}, \tilde{F}_{32}$ defined in (10).

The DEIM version of SWE model

- Let $U^{F_{11}} \in \mathbb{R}^{n_x y \times m},\ m \leq n$, be the POD basis matrix of rank m for snapshots of the nonlinear function $\tilde{F}_{11}$ (obtained from ADI FD scheme).
- Using the DEIM algorithm we select a set of m DEIM indices corresponding to $U^{F_{11}}$, denoting by $[\rho_1^{F_{11}}, .., \rho_m^{F_{11}}]^T \in \mathbb{R}^m$. The DEIM approximation of F_{11} is

$$\tilde{F}_{11} \approx U^{F_{11}} (P_{F_{11}}^T U^{F_{11}})^{-1} \tilde{F}_{11}^m,$$

so the projected nonlinear term $U^T \tilde{F}_{11}(\tilde{u}, \tilde{\phi})$ in the POD reduced system (9) can be approximated as

$$U^T \tilde{F}_{11}(\tilde{u}, \tilde{\phi}) \approx \underbrace{U^T U^{F_{11}} (P_{F_{11}}^T U^{F_{11}})^{-1}}_{E_1 \in \mathbb{R}^{k \times m}} \underbrace{\tilde{F}_{11}^m(\tilde{u}, \tilde{\phi})}_{m \times 1},$$

where $\tilde{F}_{11}^m(\tilde{u}, \tilde{\phi}) = P_{F_{11}}^T \tilde{F}_{11}(\tilde{u}, \tilde{\phi})$.

Since $\tilde{F}_{11}$ is a pointwise function, $\tilde{F}_{11}^m : \mathbb{R}^k \times \mathbb{R}^k \to \mathbb{R}^m$ can be defined as

$$\tilde{F}_{11}^m(\tilde{u}, \tilde{\phi}) = (P_{F_{11}}^T U\tilde{u}) * (\underbrace{P_{F_{11}}^T A_x U}\,\tilde{u}) + \frac{1}{2}(P_{F_{11}}^T \Phi\tilde{\phi}) * (\underbrace{P_{F_{11}}^T A_x \Phi}\,\tilde{\phi})$$

Similarly we obtain the DEIM approximation for the rest of the projected nonlinear terms in (11)

$$U^T \tilde{F}_{12}(\tilde{u}, \tilde{v}) \approx \underbrace{U^T U^{F_{12}} (P_{F_{12}}^T U^{F_{12}})^{-1}}_{E_2 \in \mathbb{R}^{k\times m}} \underbrace{\tilde{F}_{12}^m(\tilde{u}, \tilde{v})}_{m\times 1},$$

$$V^T \tilde{F}_{21}(\tilde{u}, \tilde{v}) \approx \underbrace{V^T U^{F_{21}} (P_{F_{21}}^T U^{F_{21}})^{-1}}_{E_3 \in \mathbb{R}^{k\times m}} \underbrace{\tilde{F}_{21}^m(\tilde{u}, \tilde{v})}_{m\times 1},$$

$$V^T \tilde{F}_{22}(\tilde{v}, \tilde{\phi}) \approx \underbrace{V^T U^{F_{22}} (P_{F_{22}}^T U^{F_{22}})^{-1}}_{E_4 \in \mathbb{R}^{k\times m}} \underbrace{\tilde{F}_{22}^m(\tilde{v}, \tilde{\phi})}_{m\times 1},$$

$$\Phi^T \tilde{F}_{31}(\tilde{u}, \tilde{\phi}) \approx \underbrace{\Phi^T U^{F_{31}} (P_{F_{31}}^T U^{F_{31}})^{-1}}_{E_5 \in \mathbb{R}^{k\times m}} \underbrace{\tilde{F}_{31}^m(\tilde{u}, \tilde{\phi})}_{m\times 1},$$

$$\Phi^T \tilde{F}_{32}(\tilde{v}, \tilde{\phi}) \approx \underbrace{\Phi^T U^{F_{32}} (P_{F_{32}}^T U^{F_{32}})^{-1}}_{E_6 \in \mathbb{R}^{k\times m}} \underbrace{\tilde{F}_{32}^m(\tilde{v}, \tilde{\phi})}_{m\times 1},$$

The DEIM version of SWE model

$$\begin{aligned}
\tilde{F}^m_{12}(\tilde{u},\tilde{v}) &= (P^T_{F_{12}} V\tilde{v}) * (\underbrace{P^T_{F_{12}} A_y U}\tilde{u}),\\
\tilde{F}^m_{21}(\tilde{u},\tilde{v}) &= (P^T_{F_{21}} U\tilde{u}) * (\underbrace{P^T_{F_{21}} A_x V}\tilde{v}),\\
\tilde{F}^m_{22}(\tilde{v},\tilde{\phi}) &= (P^T_{F_{22}} V\tilde{v}) * (\underbrace{P^T_{F_{22}} A_y V}\tilde{v}) + \frac{1}{2}(P^T_{F_{22}} \Phi\tilde{\phi}) * (\underbrace{P^T_{F_{22}} A_y \Phi}\tilde{\phi}),\\
\tilde{F}^m_{31}(\tilde{u},\tilde{\phi}) &= (P^T_{F_{31}} \Phi\tilde{\phi}) * (\underbrace{P^T_{F_{31}} A_x U}\tilde{u}) + (P^T_{F_{31}} U\tilde{u}) * (\underbrace{P^T_{F_{31}} A_x \Phi}\tilde{\phi}),\\
\tilde{F}^m_{32}(\tilde{v},\tilde{\phi}) &= \frac{1}{2}(P^T_{F_{32}} \Phi\tilde{\phi}) * (\underbrace{P^T_{F_{32}} A_y V}\tilde{v}) + (P^T_{F_{32}} V\tilde{v}) * (\underbrace{P^T_{F_{32}} A_y \Phi}\tilde{\phi}).
\end{aligned} \tag{13}$$

- Each of the $k \times m$ coefficient matrices grouped by the curly brackets in (13), as well as $E_i,\ i = 1, 2, .., 6$ can be precomputed and re-used at all time steps, so that the computational complexity of the approximate nonlinear terms are independent of the full-order dimension n_{xy}. Finally, the POD-DEIM reduced system for the first step of ADI FD SWE model is of the form

$$
\begin{aligned}
\tilde{u}(t_{n+\frac{1}{2}}) + \frac{\Delta t}{2} E_1 \tilde{F}_{11}^m\Big(\tilde{u}(t_{n+\frac{1}{2}}), \tilde{\phi}(t_{n+\frac{1}{2}})\Big) &= \tilde{u}(t_n) - \frac{\Delta t}{2} E_2 \tilde{F}_{12}^m\Big(\tilde{u}(t_n), \tilde{v}(t_n)\Big) \\
&\quad + \frac{\Delta t}{2} U^T A_1 \tilde{v}(t_n), \\
\tilde{v}(t_{n+\frac{1}{2}}) + \frac{\Delta t}{2} E_3 \tilde{F}_{21}^m\Big(\tilde{u}(t_{n+\frac{1}{2}}), \tilde{v}(t_{n+\frac{1}{2}})\Big) &+ \frac{\Delta t}{2} V^T A_2 \tilde{u}(t_{n+\frac{1}{2}}) \\
&= \tilde{v}(t_n) - \frac{\Delta t}{2} E_4 \tilde{F}_{22}^m\Big(\tilde{v}(t_n), \tilde{\phi}(t_n)\Big), \\
\tilde{\phi}(t_{n+\frac{1}{2}}) + \frac{\Delta t}{2} E_5 \tilde{F}_{31}^m\Big(\tilde{u}(t_{n+\frac{1}{2}}), \tilde{\phi}(t_{n+\frac{1}{2}})\Big) &= \tilde{\phi}(t_n) - \frac{\Delta t}{2} E_6 \tilde{F}_{32}^m\Big(\tilde{v}(t_n), \tilde{\phi}(t_n)\Big).
\end{aligned}
\tag{14}
$$

Numerical Results

- The domain was discretized using a mesh of 301×221 points, with $\Delta x = \Delta y = 20km$. Thus the dimension of the full-order discretized model is 66521. The integration time window was $24h$ and we used 91 time steps ($NT = 91$) with $\Delta t = 960s$.
- ADI FD scheme proposed by Gustafsson (1971) was first employed in order to obtain the numerical solution of the SWE model.
- The initial condition were derived from the geopotential height formulation introduced by Grammelvedt (1969) using the geostrophic balance relationship.

Numerical Results

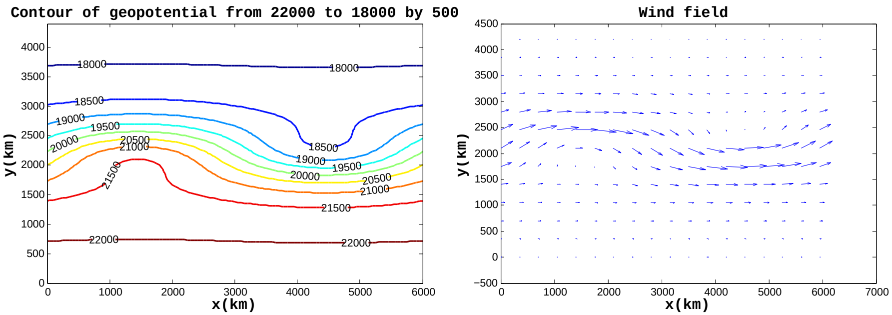

Fig.3 Initial condition: Geopotential height field for the Grammeltvedt initial condition (left). Wind field (arrows are scaled by a factor of 1km) calculated from the geopotential field by using the geostrophic approximation (right).

Numerical Results

- The implicit scheme allowed us to integrate in time using a larger time step deduced from the following Courant-Friedrichs-Levy (CFL) condition

$$\sqrt{gh}\left(\frac{\Delta t}{\Delta x}\right) < 7.188.$$

- The nonlinear algebraic systems of ADI FD SWE scheme were solved with the Quasi-Newton method and the LU decomposition was performed only once every $6 - th$ time step.

Numerical Results

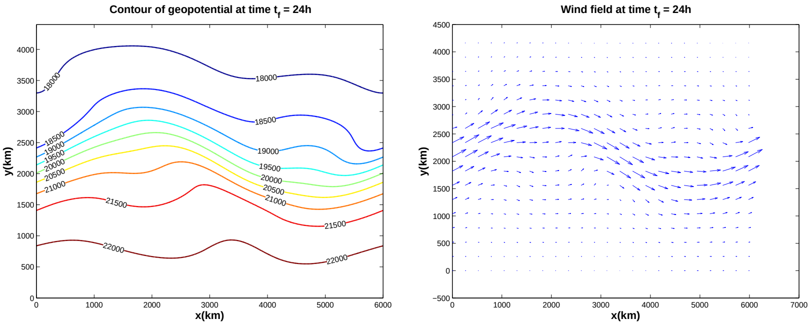

Fig.4 The geopotential field (left) and the wind field (the velocity unit is 1km/s) at $t = t_f = 24h$ obtained using the ADI FD SWE scheme for $\Delta t = 960s$.

Numerical Results

- The POD basis functions were constructed using 91 snapshots obtained from the numerical solution of the full - order ADI FD SWE model at equally spaced time steps in the interval $[0, 24h]$.
- Next figure shows the decay around the eigenvalues of the snapshot solutions for u, v, ϕ and the nonlinear snapshots F_{11}, F_{12}, F_{21}, F_{22}, F_{31}, F_{32}.

Numerical Results

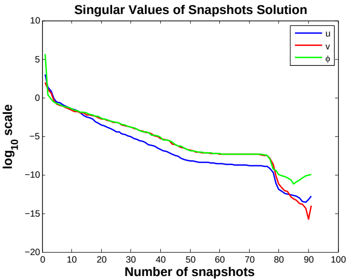

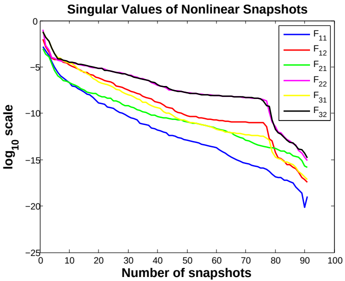

Fig.5 The decay around the singular values of the snapshots solutions for $u, v,\ \phi$ and nonlinear functions for $\Delta t = 960s$.

Numerical Results

- The dimension of the POD bases for each variable was taken to be 35, capturing more than 99.9% of the system energy.
- We applied the DEIM algorithm for interpolation indices to improve the efficiency of the POD approximation and to achieve a complexity reduction of the nonlinear terms with a complexity proportional to the number of reduced variables.
- Next image illustrates the distribution of the first 40 spatial points selected from the DEIM algorithm using the POD bases of F_{31} and F_{32} as inputs.

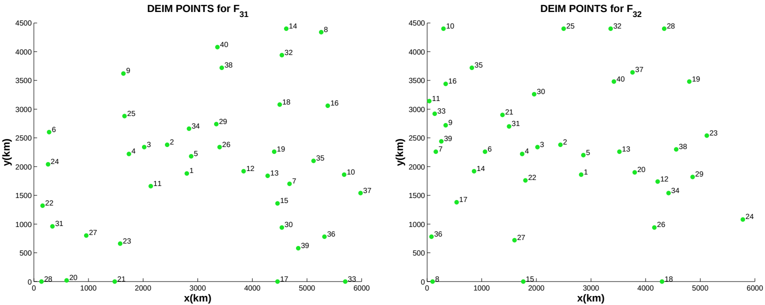

Fig.6 First 40 points selected by DEIM for the nonlinear functions F_{31} (left) and F_{32} (right)

- Using the following norms

$$\frac{1}{NT}\sum_{i=1}^{t_f}\frac{||w^{ADI\ \ FD}(:,i)-w^{POD\ \ ADI}(:,i)||_2}{||w^{ADI\ \ FD}(:,i)||_2},$$

$$\frac{1}{NT}\sum_{i=1}^{t_f}\frac{||w^{ADI\ \ FD}(:,i)-w^{POD/DEIM\ \ ADI}(:,i)||_2}{||w^{ADI\ \ FD}(:,i)||_2},$$

$i=1,2,..,t_f$ we calculated the average relative errors in Euclidian norm for all three variables of SWE model $w=u,v,\phi$.

	POD ADI SWE	POD/DEIM ADI SWE
E_ϕ	7.127e-005	1.106e-004
E_u	4.905e-003	6.189e-003
E_v	6.356e-003	9.183e-003

Table 1 Average relative errors for each of the model variables. The POD bases dimensions were taken 35 capturing more than 99.9% of the system energy. 90 DEIM points were chosen.

- We also propose an Euler explicit FD SWE scheme as the starting point for a POD, POD/DEIM reduced model. The POD bases were constructed using the same 91 snapshots as in the POD ADI SWE case, only this time the Galerkin projection was applied to the Euler FD SWE model.
- This time we employed the root mean square error calculation in order to compare the POD and POD/DEIM techniques at time $t = 24h$.

	ADI SWE	POD ADI SWE	POD/DEIM ADI SWE	POD EE SWE	POD/DEIM EE SWE
CPU time seconds	73.081	43.021	0.582	43.921	0.639
$RMSE_{\phi}$	-	5.416e-005	9.668e-005	1.545e-004	1.792e-004
$RMSE_{u}$	-	1.650e-004	2.579e-004	1.918e-004	3.126e-004
$RMSE_{v}$	-	8.795e-005	1.604e-004	1.667e-004	2.237e-004

Table 2 CPU time gains and the root mean square errors for each of the model variables at $t = t_f$. The POD bases dimensions were taken as 35 capturing more than 99.9% of the system energy. 90 DEIM points were chosen.

Numerical Results

- Applying DEIM method to POD ADI SWE model we reduced the computational time by a factor of 73.91.
- In the case of the explicit scheme the DEIM algorithm decreased the CPU time by a factor of 68.733.

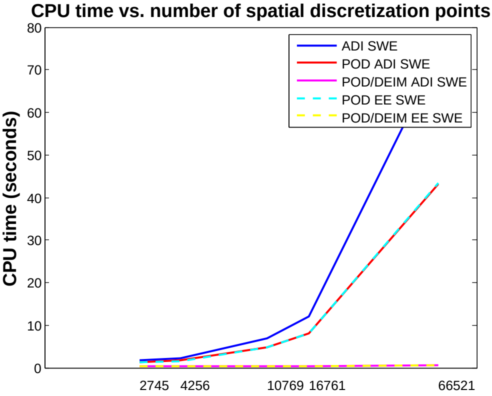

Fig.7 Cpu time vs. Spatial discretization points; POD DIM = 35, No. DEIM points = 90.

Conclusion and future research

- POD/DEIM Nonlinear model order reduction of an ADI implicit shallow water equations model, R. Stefanescu and I.M. Navon, Journal of Computational Physics, in press (2012).
- To obtain the approximate solution in case of both POD and POD/DEIM reduced systems, one must store POD or POD/DEIM solutions of order $O(kNT)$, k being the POD bases dimension and NT the number of time steps in the integration window.
- The coefficient matrices that must be retained while solving the POD reduced system are of order of $O(k^2)$ for projected linear terms and $O(n_{xy}k)$ for the nonlinear term, where n_{xy} is the space dimension.

Conclusion and future research

- In the case of solving POD/DEIM reduced system the coefficient matrices that need to be stored are of order of $O(k^2)$ for projected linear terms and $O(mk)$ for the nonlinear terms, where m is the number of DEIM points determined by the DEIM indexes algorithm, $m \ll n_{xy}$.
- Therefore DEIM improves the efficiency of the POD approximation and achieves a complexity reduction of the nonlinear term with a complexity proportional to the number of reduced variables.
- We proved the efficiency of DEIM using two different schemes, the ADI FD SWE fully implicit model and the Euler explicit FD SWE scheme.
- In future research we plan to apply the DEIM technique to different inverse problems such as POD 4-D VAR of the limited area finite element shallow water equations and adaptive POD 4-D VAR applied to a finite volume SWE model on the sphere.

Dual weighted POD in 4-D Var data assimilation

- Work of Meyer and Matthies (2003)
- Goal oriented model constrained optimization
- Bui-Thanh et al. (2007)
- We aim to incorporate data assimilation system (DAS) into model reduction
- We propose a dual-weighted POD method (DW POD)
- Combine info from both model dynamics and DAS
- Data weighting in POD, considered by Graham and Kevrekidis (1996)
- Kunisch and Volkwein (2002) use time distribution of snapshots

I.M. Navon, R. Ştefănescu

POD History

POD Galerkin reduced order model

POD definition

POD/DEIM POD/EIM justification and methodology

POD/DEIM nonlinear model reduction for SWE

POD/DEIM as a discrete variant of EIM and their pseudo - algorithms

Dual weighted POD in 4-D Var data assimilation

Proper orthogonal decomposition of structurally dominated turbulent flows

Trust Region POD 4-D VAR of the limited area FEM SWE

Dual weighted POD in 4-D Var data assimilation

- Start by defining weighted ensemble average of the data

$$\bar{\mathbf{x}} = \sum_{i=1}^{i=n} w_i \mathbf{x}^i,$$

with the snapshots weights $w_i \in (0,1)$ and $\sum_{i=1}^{n} w_i = 1$.
- They assign degree of importance to each member of the assemble
- In standard approach $w_i = \frac{1}{n}$.
- The modified $m \times n$ matrix obtained by subtracting the mean from each snapshot is

$$\mathbf{X} = [\mathbf{x}^1 - \bar{\mathbf{x}}, \mathbf{x}^2 - \bar{\mathbf{x}}, \ldots, \mathbf{x}^n - \bar{\mathbf{x}}]$$

- Weighted covariance matrix $\mathbf{C}\imath\mathbb{R}^{m\times m}$

$$\mathbf{C} = \mathbf{X}\mathbf{W}\mathbf{X}^{\mathbf{T}}$$

where

$$W = \mathrm{diag}[w_1, .., w_n].$$

Dual weighted POD in 4-D Var data assimilation

- We consider general norm

$$||\mathbf{X}||_{\mathbf{A}}^2 = \langle \mathbf{x}, \mathbf{x} \rangle_{\mathbf{A}} = \mathbf{x}^{\mathbf{T}} \mathbf{A} \mathbf{x},$$

$A \in \mathbb{R}^{m \times m}$ is s.p.d.

- POD basis of order $k \leq n$ minimizes the averaged projection error

$$\min_{\{\psi^1, \psi^2, \ldots, \psi^k\}} \sum_{i=1}^{n} w_i \left\| \left(\mathbf{x}^i - \bar{\mathbf{x}}\right) - P_{\Psi,k}\left(\mathbf{x}^i - \bar{\mathbf{x}}\right) \right\|_2^2$$

s.t. A orthonormality constraint $\left\langle \psi^i, \psi^j \right\rangle_{l_2} = \delta_{ij}$ and $P_{\Psi,k}$ is the projection operator onto the $k-$dimensional space $\mathrm{Span}\left\{\psi^1, \psi^2, \ldots, \psi^M\right\}$

$$P_{\Psi,k}(\mathbf{x}) = \sum_{i=1}^{k} \langle \mathbf{x}, \psi_i \rangle_A \psi_i.$$

Dual weighted POD in 4-D Var data assimilation

- POD modes $\psi_i \in \mathbb{R}^m$ are eigenvectors of m dimensional eigenvalue problem

$$\mathbf{CA}\psi^i = \sigma_i^2 \psi_i$$

- Compute

$$\mathbf{W}^{1/2}\mathbf{X}^\mathbf{T}\mathbf{A}\mathbf{X}\mathbf{W}^{1/2}\mu_i = \sigma_i^2 \mu_i$$

  1. **A** is identity for Euclidian norm
  2. **A** is diagonal for total energy metric

- Once we obtain eigenvectors $\mu_i \in \mathbb{R}^n$ orthonormal w.r.t. Euclidian norms, compute the POD modes

$$\psi_i = \frac{1}{\sigma_i}\mathbf{X}\mathbf{W}^{\frac{1}{2}}\mu_i.$$

Reduced-order 4D-Var

- The k-dimensional reduced-order control problem is obtained by projecting $\mathbf{x_0} - \bar{\mathbf{x}}$ on the POD space

$$P_{\mathbf{\Psi},\mathbf{k}}(\mathbf{x_0} - \bar{\mathbf{x}}) = \mathbf{\Psi}_\eta = \sum_{i=1}^{k} \eta_i \psi_i$$

where matrix

$$\mathbf{\Psi} = [\psi_1, .., \psi_k] \in \mathbb{R}^{m \times k}$$

has the POD basis vectors as columns, and $\eta = (\eta_1, .., eta_k)^T \in \mathbb{R}^k$ is the coordinate vector in reduced space

$$\eta_i = \psi_i^T \mathbf{A}(\mathbf{x_0} - \bar{\mathbf{x}})$$

$$\boldsymbol{\eta} = \mathbf{\Psi}^T \mathbf{A}(\mathbf{X_0} - \bar{\mathbf{X}})$$

Reduced-order 4D-Var

- Large scale 4-D Var optimization

$$\min_{\mathbf{x_0}\in\mathbb{R}^m} J(\mathbf{x_0})$$

for $\mathbf{x_0}^a = \text{argmin } J$.

$$J = \frac{1}{2}(\mathbf{x_0}-\mathbf{x_b})^T\mathbf{B}^{-1}(\mathbf{x_0}-\mathbf{x_b})$$

$$+\frac{1}{2}\sum_{k=0}^{k=N}(H_k\mathbf{x_k}-y_k^o)^{\mathbf{T}}\mathbf{R}_k^{-1}(H_k\mathbf{x_k}-y_k^o)$$

- **B** background error covariance matrix
- $\mathbf{R}_k$ observation error covariance matrix at time level k
- H_k observation operator at time level k which has linear representation
- $\mathbf{x_0}$ control variables vector represented by POD basis
- $\mathbf{x}_k$ vector of variables obtained from the reduced-order model at the time level k

Reduced-order 4D-Var

- It is now replaced by reduced-order 4D-Var of finding optimal coefficients $\boldsymbol{\eta}$ s.t.

$$\hat{J}(\boldsymbol{\eta}) = J(\mathbf{x} + \boldsymbol{\Psi}\boldsymbol{\eta}) \text{ and } \min_{\boldsymbol{\eta} \in \mathbb{R}^k} \hat{J}(\boldsymbol{\eta}).$$

- If $\boldsymbol{\eta}^a$ denotes solution of this problem, an approximation to analysis $(*)$ is given by

$$\mathbf{x}_0^a \simeq \bar{\mathbf{x}} + \boldsymbol{\Psi}\boldsymbol{\eta}^a.$$

- Only the initial conditions are projected into the POD space and cost functional is computed using the full-model dynamics

$$\nabla_{\boldsymbol{\eta}} \hat{J}(\boldsymbol{\eta}) = \boldsymbol{\Psi}^T (\nabla_{\mathbf{x}_0} J)|_{\mathbf{x}_0} = \bar{\mathbf{x}} + \boldsymbol{\Psi}\boldsymbol{\eta},$$

Reduced-order 4D-Var

- For any fixed time instant $\tau < t$, we have $\mathbf{x}(t) = \mathcal{M}_{\tau,t}[\mathbf{x}(\tau)]$.
- We make use of time-varying sensitivities of 4-D Var functional w.r.t. perturbations in the state at time instants t_i, $i = 1, 2, .., n$ where snapshots are taken.
- We can estimate impact of perturbation δx_i in state vector at snapshot time $t_i \leq t$ on J using the TLM model $M(t_i, t)$ and its adjoint model $M^*(t, t_i)$

$$\nabla J \simeq < \nabla_{\mathbf{x}(t)} J[\mathbf{x}(t)], \boldsymbol{\delta}\mathbf{x}(t) > = \nabla_{\mathbf{x}(t)} J[\mathbf{x}(t)], M(t_i, t)\boldsymbol{\delta}\mathbf{x}(t_i) >$$

$$= < M^*(t, t_i)\nabla_{\mathbf{x}(t)} J[\mathbf{x}(t)], \boldsymbol{\delta}\mathbf{x}(t_i) > = < \boldsymbol{\lambda}(t_i), \boldsymbol{\delta}\mathbf{x}(t_i) > .$$

Reduced-order 4D-Var

- where $\boldsymbol{\lambda}(t_i) \in \mathbb{R}^m,\ \boldsymbol{\lambda}(t_i) = M^*(t, t_i)\nabla_{\mathbf{x}(t)} J[\mathbf{x}(t)]$ are the adjoint state variables at time t_i.
- It follows

$$|\delta J| \simeq |<\boldsymbol{\lambda}(t_i), \delta\mathbf{x}(t_i)>| = |<\mathbf{A}^{-1}\boldsymbol{\lambda}(t_i), \delta\mathbf{x}(t_i)>_{\mathbf{A}}|$$

$$\leq ||\mathbf{A}^{-1}\boldsymbol{\lambda}(t_i)||_{\mathbf{A}} ||\delta\mathbf{x}(t_i)||_{\mathbf{A}}$$

- The dual weights w_i corresponding to the snapshots are defined as normalized values

$$\alpha_i = ||\mathbf{A}^{-1}\boldsymbol{\lambda}(t_i)||_{\mathbf{A}} \text{ and } w_i = \frac{\alpha_i}{\sum_{j=1}^{n}\alpha_j}, \text{ for } i = 1, 2, .., n.$$

Reduced-order 4D-Var

- They provide a measure of relative impact of the state errors $||\delta \mathbf{x}(t_i)||_{\mathbf{A}}$ on the cost functional.
- The weights are determined by the cost functional s.t. information from DAS is incorporated directly into the optimality criteria.
- This is a time - targeting assigning weights to time distributed snapshot data using a time-varying adjoint sensitivity field.
- It requires (evaluation of all dual weights) only one adjoint model integration.

$$\boldsymbol{\lambda}(t_{N+1}) = 0$$

$$\boldsymbol{\lambda}(t_k) = M^*(t_{k+1}, t_k)\boldsymbol{\lambda}(t_{k+1}) + \mathbf{H}_k^T \mathbf{R}_k^{-1}(\mathbf{H}_k \mathbf{x}_k - \mathbf{y}_k)$$

$$\text{for } k = N, N-1, .., 0, \text{ and}$$

$$\boldsymbol{\lambda}(t_0) = \boldsymbol{\lambda}(t_0) + \mathbf{B}^{-1}(\mathbf{x}_0 - \mathbf{x}_b)$$

Numerical Experiments

- Uses 2-D S-W equations model on the sphere using the explicit flux form semi-Lagrangian (FF-SL) scheme
- Adjoint developed by Akella and Navon (2006) using TAMC (Giering and Kaminski, 1998) AD Software
- We consider a total energy norm

$$||\mathbf{x}||^2_{\mathbf{A}} = \frac{1}{2}(||u||^2 + ||v||^2 + \frac{g}{\bar{h}}||h||^2),$$

where $\bar{h}$ is the mean height of the reference data.

Results

- DAS-I - data provided for all discrete state components - no background term included.
- DAS-II - background term included, data provided every fourth grid point in longitudinal and latitudinal directions

Results

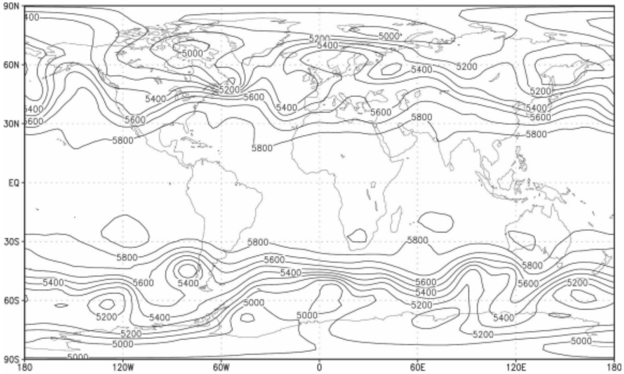

Fig.8 Isopleths of the geopotential height (m) for the reference run: configuration at the initial time specified from ERA-40 datasets;

Results

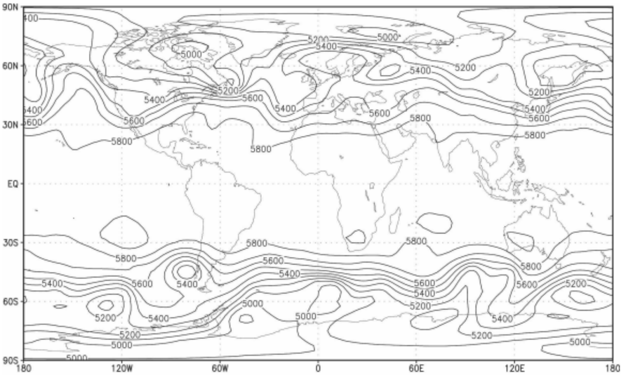

Fig.9 Isopleths of the geopotential height (m) for the reference run: the 24-h forecast of the shallow-water model.

Results

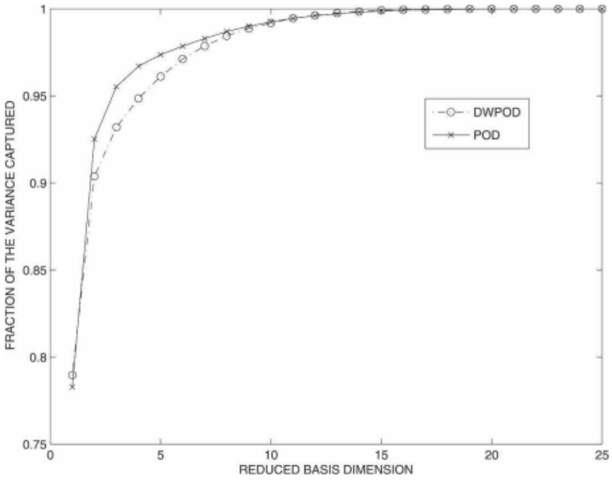

Fig.10 The fraction of the variance captured by the POD and DWPOD modes from the snapshot data as a function of the dimension of the reduced space.

Results

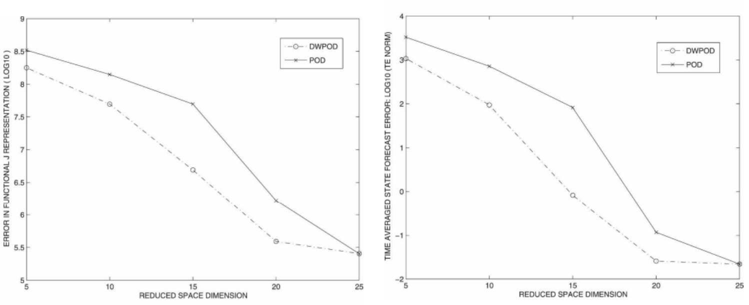

Fig.11 Comparative results for the reduced-order POD and DWPOD forecasts as the dimension of the reduced space varies for k = 5, 10, 15, 20, and 25. (left) Error (log 10) in the reduced order representation of the time-integrated total energy of the system. (right) Time-averaged state forecast error (log 10).

Results

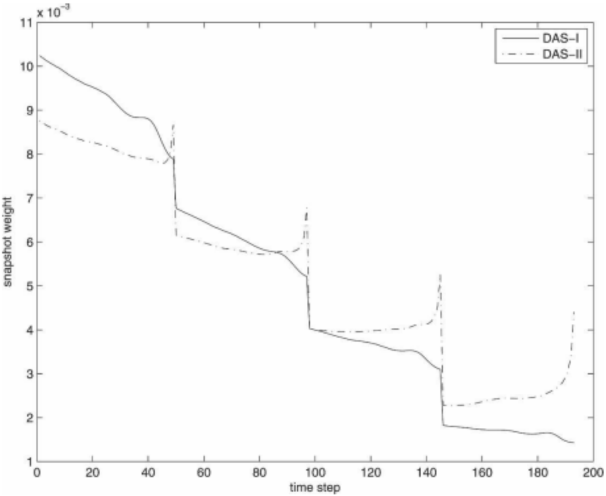

Fig.12 The dual weights for the snapshot data determined by the adjoint model in DAS-I and in DAS-II.

Results

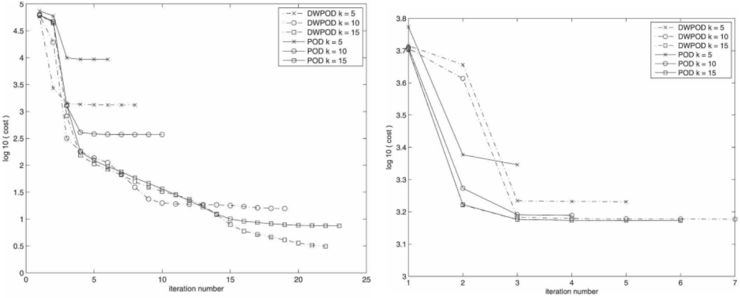

Fig.13 The iterative minimization process in the reduced space for the POD and DWPOD spaces of dimension 5, 10, and 15. (left) Optimization without background term and dense observations, corresponding to DAS-I. (right) Optimization with background term and sparse observations, corresponding to DAS-II

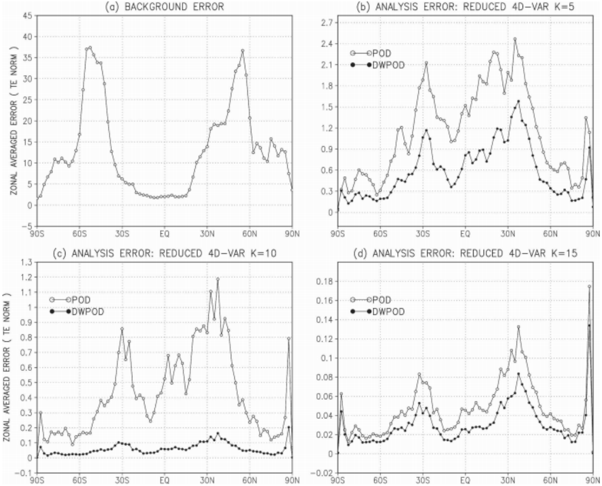

Fig.14 Zonally averaged errors ($m^2\ s^{-2}$) in the background estimate and in the analysis provided by the reduced-order 4DVAR data assimilation. Results for the DAS-I experiments with POD and DWPOD spaces of dimension 5, 10, and 15.

Conclusions

- Beneficial results for use with small dimensional bases in context of adaptive order reduction as minimization approaches optimal solution.
- Increase accuracy using DWPOD in representation of forecast aspect by one order of magnitude

Proper orthogonal decomposition of structurally dominated turbulent flows

- The POD/Galerkin finite-element model (FEM) lacks stability and spurious oscillations can degrade the reduced order solution for flows with high Reynolds numbers.
- The instabilities commonly observed in the POD method are due to the oscillations forming in the solutions as a result of applying a standard Bubnov-Galerkin projection of the equations onto the reduced order sapce.
- These oscillations feed into the nonlinear terms at moderate to high Reynolds number resulting in unstable simulations.
- We address one specific way for turbulence closure the Petrov-Galerkin projection with ROM

Proper orthogonal decomposition of structurally dominated turbulent flows

- The reason for the inadequate behavior of POD-Galerkin truncation is that although the discarded POD modes $\{\Phi_{r+1}, .., \Phi_d\}$ do not contain a significant amount of kinetic energy in the system, they do however have a significant role in the dynamics of the reduced-order system.
- Indeed, the interaction between the discarded POD modes $\{\Phi_{r+1}, .., \Phi_d\}$ and the POD modes retained in the ROM $\{\Phi_1, .., \Phi_r\}$ is essential for an accurate prediction of th dynamics of the ROM.
- This situation is similar to the traditional Fourier setting for turbulence, in which the effect of the discard Fourier modes needs to be modeled, i.e. one needs to solve the celebrated closure problem.
- This similarity is not surprising since in the limit of homogeneous flows the POD basis reduces to the Fourier basis (Holmes et al. 1996, 2012).

Proper orthogonal decomposition of structurally dominated turbulent flows

- It was recognized early that a simple Galerkin truncation of POD basis will generally produce inaccurate results no matter that the retained POD modes capture most of the system energy
- Various closure methods have been proposed.
- Basic work of Kunisch and Volkwein (1999,2002)
- Calibration methods Galetti (1986,1987)
- State calibration method and flow calibration method Couplet (2004).

Other methods

- Numerical stability enhancing closure models
- Sirisup and Karniadakis (2005) show that onset of divergence from correct limit cycle depends on number of modes in the Galerkin expansion, The Reynolds number and the flow geometry
- Replacing L^2 inner product with the H^1 inner product Gradient information is also incorporated in the POD modes
- Bergman et al (2009) used streamline upwind Petrov-Galerkin method
- Closure models based on physical input (addition of eddy viscosity) by Aubry et al. 1988

Petrov-Galerkin method

- Many stabilization methods involve optimization of many parameters to achieve a required accuracy.
- Recently Carlberg et al (2011) introduced the Petrov Galerkin method to control the stability of a 1-D nonlinear static problem
- The Petrov-Galerkin method offers a natural and easy way to introduce a diffusion term into ROM without tuning optimization.

Petrov-Galerkin method

- In Fang et al. (2012), a new Petrov-Galerkin method is used for stabilization of reduced order modeling of a nonlinear hybrid unstructured mesh applied to the Navier-Stokes equations.
- A mixed $P_{1DG}P_2$ FEM pair (Cotter et al. 2009) which remains LBB stable is introduced to further stabilize the numerical oscillations.
- It consists of discontinuous linear elements for velocity and continuous quadratic elements for pressure in the Navier-Stokes equations.

Petrov-Galerkin ROM

- The Petrov-Galerkin method is used to form a stable POD ROM for nonlinear hybrid problems.
- At a given time step the discretization of the Navier-Stokes equations has the form

$$\mathbf{A}\Psi = \mathbf{b}, \tag{15}$$

where

$$\Psi = (\mathbf{U}, \mathbf{V}, \mathbf{W}, \mathbf{P})^T, \quad \mathbf{U} = (u_1, \dots, u_i, \dots, u_{\mathcal{N}}),$$

$$\mathbf{V} = (v_1, \dots, v_i, \dots, v_{\mathcal{N}}), \quad \mathbf{W} = (w_1, \dots, w_i, \dots, w_{\mathcal{N}})$$

$$\mathbf{P} = (p_1, \dots, p_i, \dots, p_{\mathcal{N}})$$

($\mathcal{N}$ is the number of nodes in the computational domain).

Petrov-Galerkin ROM

- A modified system of equations (15) is written as

$$\mathbf{C}^T\mathbf{F}^{-1}\mathbf{A}\Psi = \mathbf{C}^T\mathbf{F}^{-1}\mathbf{b}, \qquad (16)$$

  in which for the least squares (LS) methods,

$$\mathbf{C} = \mathbf{A}$$

- The solution of (16) is the same as that of equation (15), but it is not the same when ROM is applied.

Petrov-Galerkin ROM

- $F-$the weighting matrix can be chosen to render the system of equations dimensionally consistent and contains also the mass matrix of system.
- The LS methods have dissipative properties but are not generally conservative for coupled systems of equations.
- A common solution to divergence of ROM solutions is to add diffusion terms to the equations and tune these diffusion terms to best match the full forward solution.
- It seems natural to explore using the above Petrov-Galerkin methodology to introduce diffusion into ROM's and avoid this tuning.

Petrov-Galerkin ROM

- The matrix equation (15) can be converted into a reduced order system spanned by a set of m POD basis functions $\{\Phi_1, \ldots, \Phi_M\}$ where each POD function is represented by a vector of size $\mathcal{N}$ that represents the functions over the FEM space.
- The POD functions are grouped into a matrix $\mathbf{M}^{POD}$ of size $\mathcal{N} \times \mathcal{M}$

$$\mathbf{M}^{POD} = [\Phi_1, \ldots, \Phi_M]$$

- Using this matrix, the reduced order system can now be generated by operating directly on the discretised system given by equation (15).

Petrov-Galerkin ROM

- The standard Galerkin is resulting in the ROM system,

$$\mathbf{M}^{POD^T}\mathbf{A}\mathbf{M}^{POD}\Psi^{POD} = \mathbf{M}^{POD^T}(\mathbf{b} - \mathbf{A}\bar{\Psi}), \qquad (17)$$

where Ψ^{POD} are the reduced order solution coefficients, $\bar{\Psi}$ is the mean of the variables Ψ over the time, and the relationship between the POD variables and full solutions is given by,

$$\Psi = \mathbf{M}^{POD^T}(\Psi^{POD} + \bar{\Psi}) \qquad (18)$$

Petrov-Galerkin ROM

- For LS methods, equation (17) is:

$$\mathbf{M}^{POD^T}\mathbf{C}^T\mathbf{F}^{-1}\mathbf{A}\mathbf{M}^{POD}\Psi^{POD} = \mathbf{M}^{POD^T}\mathbf{C}^T\mathbf{F}^{-1}(\mathbf{b}-\mathbf{A}\bar{\Psi}). \quad (19)$$

and using the non-linear Petrov-Galerkin methods one obtains:

$$\mathbf{M}^{POD^T}(\mathbf{I}+\mathbf{C}^T\mathbf{F}^{-1})\mathbf{A}\mathbf{M}^{POD}\Psi^{POD} = \mathbf{M}^{POD^T}(\mathbf{I}+\mathbf{C}^T\mathbf{F}^{-1})(\mathbf{b}-\mathbf{A}\bar{\Psi}), \quad (20)$$

or in a diffusion form:

$$(\mathbf{M}^{POD^T}\mathbf{A}\mathbf{M}^{POD} + \mathbf{D})\Psi^{POD} = \mathbf{M}^{POD^T}(\mathbf{b} - \mathbf{A}\bar{\Psi}). \quad (21)$$

Petrov-Galerkin ROM

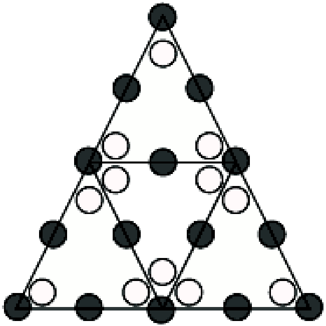

Fig.15 a mixed finite element $P_{1DG}P_2$ pair for velocity and pressure (white one for u nodes, black one for p nodes)

Petrov-Galerkin ROM

- Example I: 2D-Navier-Stokes flow past a cylinder
- Example II: Gyre problem
- Example III: Sod shock tube problem
- Example IV: 2D Advection

I.M. Navon, R. Ştefănescu

Petrov-Galerkin ROM

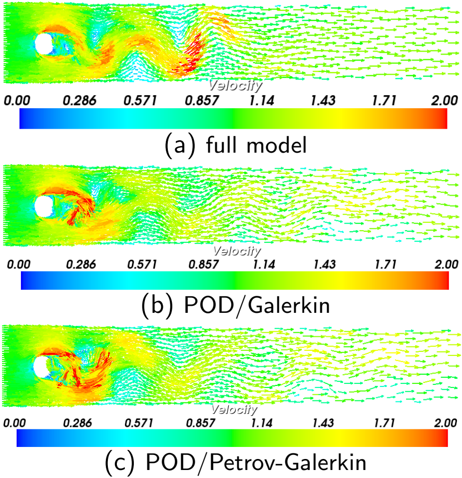

Fig.16 Flow past a cylinder: Velocity solution from the full, POD/Galerkin and POD/Petrov-Galerkin models using P_1P_1 ($t = 3.6$, $Re = 2000$).

Petrov-Galerkin ROM

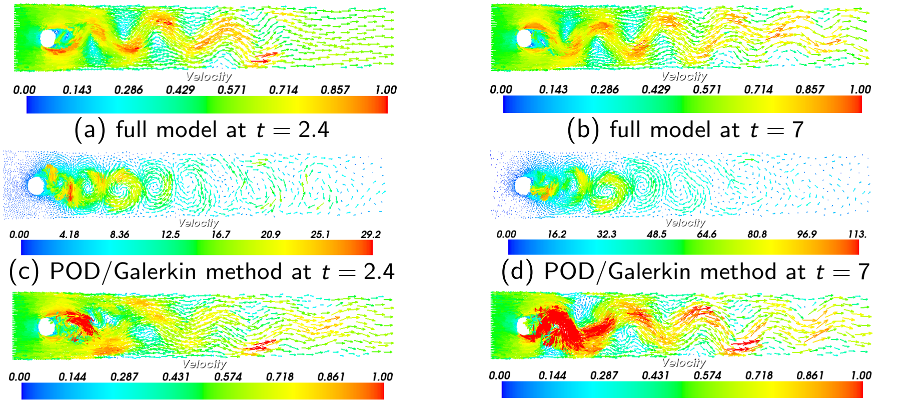

(a) full model at $t = 2.4$ (b) full model at $t = 7$

(c) POD/Galerkin method at $t = 2.4$ (d) POD/Galerkin method at $t = 7$

(e) POD/Petrov-Galerkin method at $t = 2.4$ (f) POD/Petrov-Galerkin method at $t = 7$

Fig.17 Flow past a cylinder: Velocity solution from the full, POD/Galerkin and POD/Petrov-Galerkin models using P_1P_1 at $t = 2.4$ and $t = 7$ ($Re = 3600$).

Petrov-Galerkin ROM

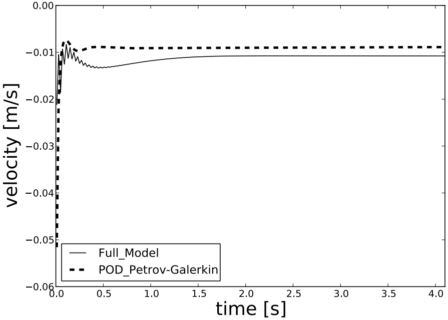

Fig.18 Comparison of velocity results between the full and Petrov-Galerkin POD models at a point(near right side of the circle).

Petrov-Galerkin ROM

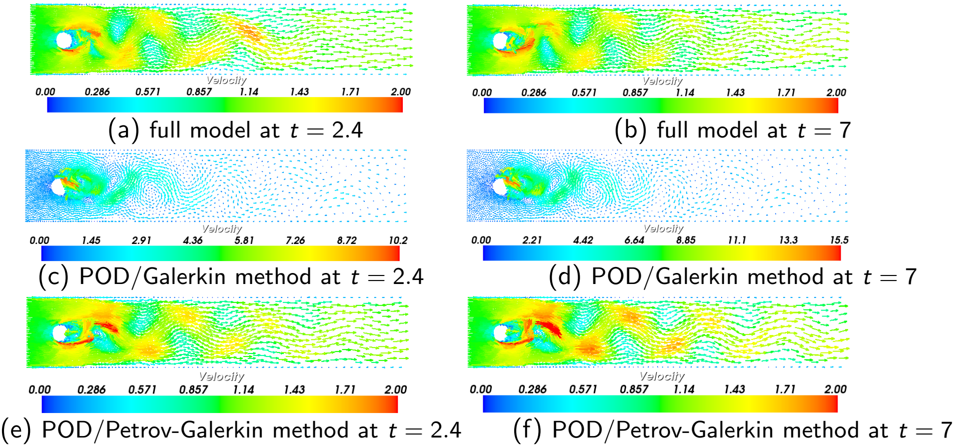

(a) full model at $t = 2.4$

(b) full model at $t = 7$

(c) POD/Galerkin method at $t = 2.4$

(d) POD/Galerkin method at $t = 7$

(e) POD/Petrov-Galerkin method at $t = 2.4$

(f) POD/Petrov-Galerkin method at $t = 7$

Fig.19 Flow past a cylinder: solution of full model, POD/Galerkin and POD/Petrov-Galerkin using $P_{1DG}P_2$ at $t = 2.4$ and $t = 7$ ($Re = 3600$)

Petrov-Galerkin ROM

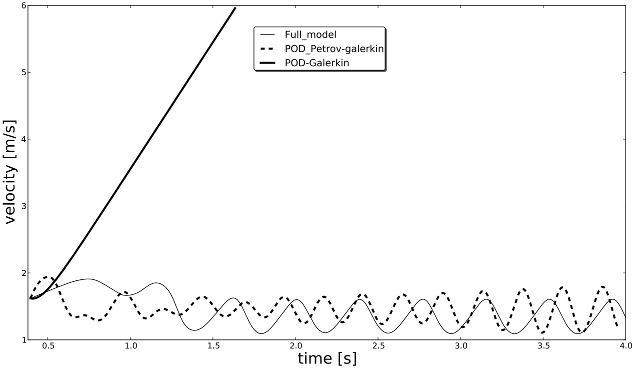

Fig.20 The comparison of velocity solution at point (x=0.3,y=0.3) between the Galerkin/POD model and Petrov-Galerkin/POD model using $P_{1DG}P_2$.

Petrov-Galerkin ROM

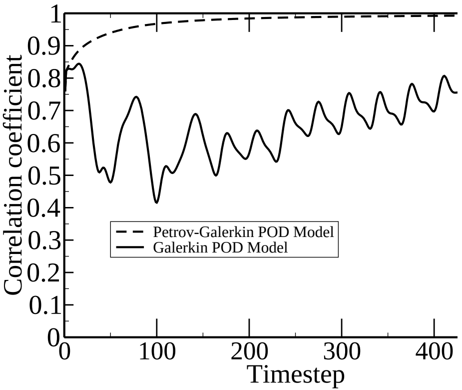

Fig.21 The correlation coefficient of the Galerkin/POD and Petrov-Galerkin/POD models using a mixed finite element $P_{1DG}P_2$ pair for velocity and pressure.

Petrov-Galerkin ROM

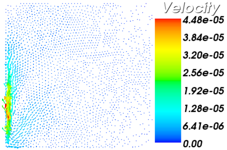

(a) full model velocity

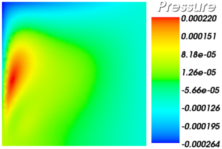

(b) full model pressure

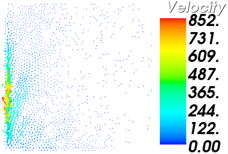

(c) POD/Galerkin method velocity

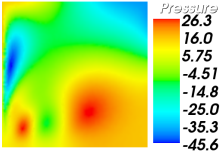

(d) POD/Galerkin method pressure

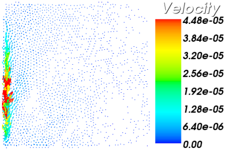

(e) POD/Petrov-Galerkin method velocity

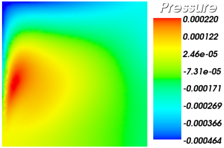

(f) POD/Petrov-Galerkin method pressure

Fig.22 Gyre: Comparison of the results between the full and POD models at $t = 0.35$ using $P_{1DG}P_2$.

I.M. Navon, R. Ştefănescu

Petrov-Galerkin ROM

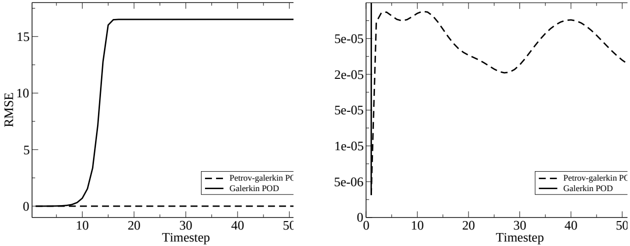

Fig.23 Gyre:RMSE between Full model and POD model; (a) RMSE of Galerkin and Petrov-Galerkin; (b) Amplification of the lower part of figure 9(a)

Petrov-Galerkin ROM

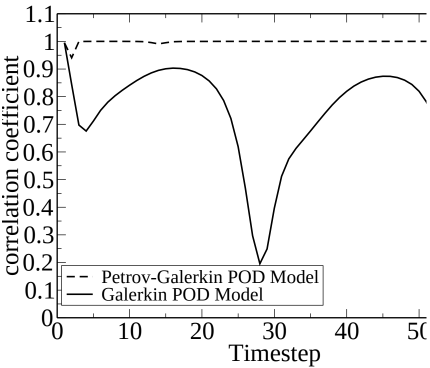

Fig.24 Correlation coefficient of Galerkin/POD model and Petrov-Galerkin/POD model.

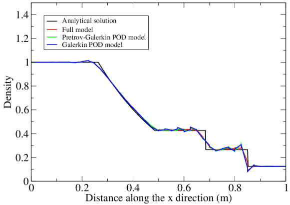

(a) Density

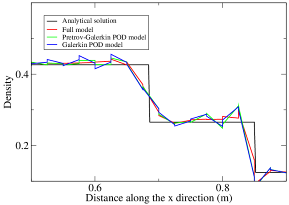

(b) Density

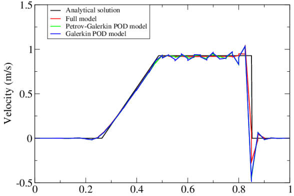

(c) Velocity

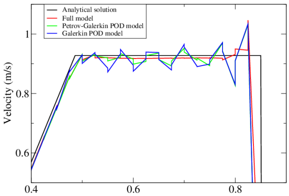

(d) Velocity

Fig.25 The Sod shock tube problem: Comparison of the results obtained from the POD and full model at time level $t = 0.2\,s$ (where 15 POD bases are used to represent 95% of the original energy).

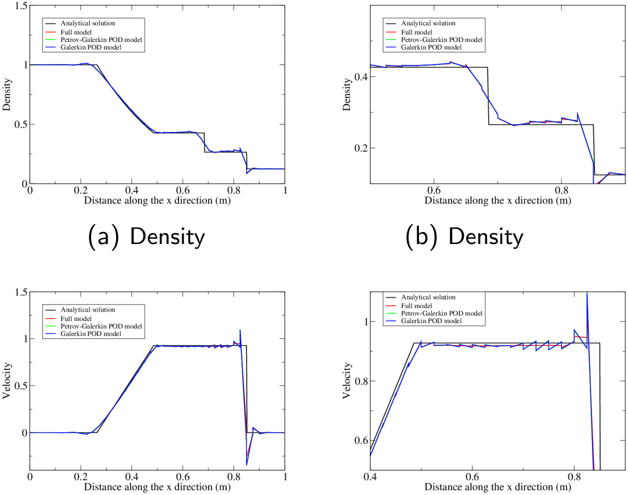

(a) Density (b) Density

(c) Velocity (d) Velocity

Fig.26 The Sod shock tube problem: Comparison of the results obtained from the POD and full model at time level $t = 0.2\,s$ (where 25 POD bases are used to represent 99.4% of the original energy).

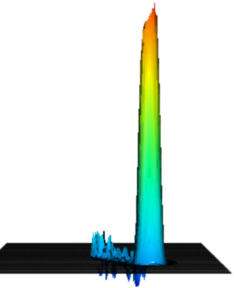

(a) Galerkin POD model at $t = 0.2\,s$

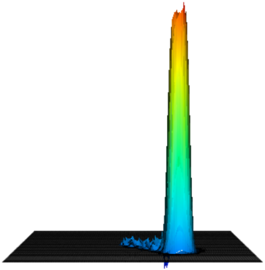

(b) Petrov-Galerkin POD model at $t = 0.2\,s$

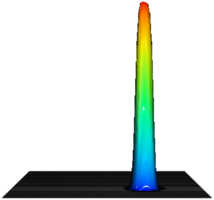

(c) Full model at $t = 0.2\,s$

Fig.27 2D 45^o advection: Comparison of the results obtained from the POD models and full model, where 15 POD bases are used, which represent 95% of the original energy.

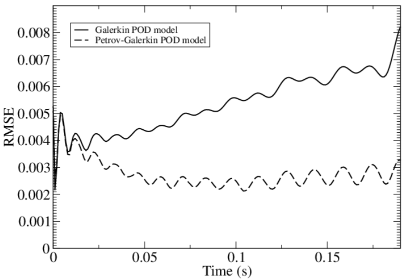

(a) RMSE (10 POD base)

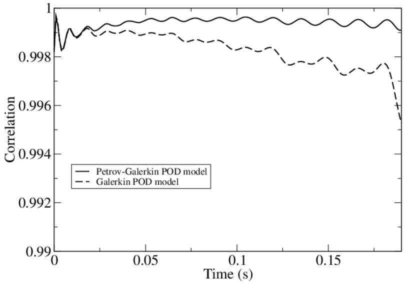

(b) Correlation (10 POD bases)

Fig.28 2D 45^o advection: RMSE and correlation coefficient of tracer results between the POD and the full models

Limited - Area SWE

- The shallow - water equations model on a $\beta-$plane

$$\frac{\partial u}{\partial t} + u\frac{\partial u}{\partial x} + v\frac{\partial u}{\partial y} + \frac{\partial \phi}{\partial x} - fv = 0$$

$$\frac{\partial v}{\partial t} + u\frac{\partial v}{\partial x} + v\frac{\partial v}{\partial y} + \frac{\partial \phi}{\partial y} + fu = 0$$

$$\frac{\partial \phi}{\partial t} + u\frac{\partial \phi}{\partial x} + v\frac{\partial \phi}{\partial y} + \phi\frac{\partial u}{\partial x} + \phi\frac{\partial v}{\partial y} = 0$$

$$(x, y) \in [0, L] \times [0, D], \quad t \geqslant 0$$

where L and D are the dimensions of a rectangular domain of integration, u and v are the velocity components in the x and y axis respectively, $\phi = gh$ is the geopotential height, h is the depth of the fluid and g is the acceleration of gravity.

Limited - Area SWE

- The scalar function f is the Coriolis parameter.

$$f = \hat{f} + \beta\left(y - \frac{D}{2}\right),\ \beta = \frac{\partial f}{\partial y}$$

- The $\hat{f}$ is the Coriolis frequency

$$f = \hat{f} + \beta\left(y - \frac{D}{2}\right)$$

- The Coriolis parameter

$$\hat{f} = 2\Omega \sin\theta$$

is defined at a mean latitude θ_0, where Ω is the angular velocity of the earth's rotation and θ is latitude.

Limited - Area SWE

- We impose initial conditions

$$w(x, y, 0) = \varphi(x, y), \text{ where state variables are}$$

$$w = w(x, y, t) = (u(x, y, t), v(x, y, t), \phi(x, y, t)),$$

with periodic boundary conditions are assumed in the x-direction:

$$w(0, y, t) = w(L, y, t)$$

whereas solid wall boundary condition are used in y-direction:

$$v(x, 0, t) = v(x, D, t) = 0.$$

POD version of SWE

- To obtain a reduced model, we first employ a FEM scheme to solve the PDE. Then we obtain an ensemble of snapshots and use a Galerkin projection scheme of the model equations onto the space spanned by the POD basis elements.
- A system of ODE is obtained as follows

$$\frac{d\alpha_i}{dt} = \left\langle F\left(\bar{y}^h + \sum_{i=1}^{i=M} \alpha_i \psi_i^h, t\right), \psi_i^h \right\rangle$$

with i.c.

$$\alpha_i(0) = \left\langle y^h(x,0) - \bar{y}^h, \psi_i^h \right\rangle = \langle y_0 - \bar{y}, \psi_i \rangle_{\mathbf{A}}, \quad i = 1, \cdots,$$

Reduced order POD 4-D VAR

- We project the control variable on a basis of characteristic vectors capturing most of the energy and main directions of variability of the model, i.e. SVD.
- We then attempt to control the vector of initial conditions in the reduced space model

$$J^{POD}\left(y_0^{POD}\right) = \frac{1}{2}\left(y_0^{POD} - y^b\right)^{\mathbf{T}} \mathbf{B}^{-1}\left(y_0^{POD} - y^b\right) +$$

$$\frac{1}{2}\sum_{k=0}^{k=n}\left(H_k y_k^{POD} - y_k^o\right)^{\mathbf{T}} \mathbf{R}_k^{-1}\left(H_k y_k^{POD} - y_k^o\right)$$

- $\mathbf{B}$ background error covariance matrix
- $\mathbf{R}_k$ observation error covariance matrix at time level k
- H_k observation operator at time level k
- y_0^{POD} vector of control variables (initial conditions) represented by POD basis
- y_k^{POD} vector of variables obtained from the reduced-order model at the time level k

Reduced order POD 4-D VAR

- The initial value y_0^{POD} and the reduced-order model solution y_k^{POD} can be expressed as

$$y_0^{POD} = \bar{y} + \sum_{i=1}^{i=M} \alpha_i(0)\,\psi_i = \bar{y} + \Psi\alpha_0$$
$$y_k^{POD} = \bar{y} + \sum_{i=1}^{i=M} \alpha_i\left(t^k\right)\psi_i = \bar{y} + \Psi\alpha_k$$

where $\Psi = \left\{\psi^1, \psi^2, \ldots, \psi^M\right\}$ is an ensemble of POD basis.

Reduced order POD 4-D VAR

- We can rewrite the reduced - order cost functional as follows

$$J_{\alpha}^{POD}(\alpha_0) = \frac{1}{2}\left(\bar{y} + \Psi\alpha_0 - y^b\right)^{\mathbf{T}} \mathbf{B}^{-1}\left(\bar{y} + \Psi\alpha_0 - y^b\right) +$$

$$\frac{1}{2}\sum_{k=0}^{k=n}\left(H_k\left(\bar{y} + \Psi\alpha_k\right) - y_k^o\right)^{\mathbf{T}} \mathbf{R}_k^{-1}\left(H_k\left(\bar{y} + \Psi\alpha_k\right) - y_k^o\right)$$

- The reduced model can be written as

$$\alpha_k = M_{0\to k}^{POD}(\alpha_0), \forall k$$

$$\alpha_k = M_{k-1\to k}^{POD}(\alpha_{k-1}) = M_k^{POD}(\alpha_{k-1}), \forall k$$

and by recurrence

$$\alpha_k = M_k^{POD} \cdots M_1^{POD}\alpha_0, \ \forall k$$

Reduced order POD 4-D VAR

- The reduced-order cost functional $J_{\alpha}^{POD}(\alpha_0)$ can be divided into two components

$$J_{\alpha}^{POD} = J_{\alpha}^{POD,b} + J_{\alpha}^{POD,o}$$

and more,

$$J_{\alpha}^{POD} = J_{\alpha}^{POD,b} + \sum_{k=0}^{n} J_{\alpha,k}^{POD,o}$$

where $J_{\alpha,k}^{POD,o} = \left(H_k\left(\bar{y} + \Psi\alpha_k\right) - y_k^o\right)^{\mathbf{T}} d_k$ and d_k denotes the 'normalized departure'

$$d_k = \mathbf{R}_k^{-1}\left(H_k\left(\bar{y} + \Psi\alpha_k\right) - y_k^o\right).$$

Reduced order POD 4-D VAR

- Hence the gradient of the POD reduced-order cost functional w.r.t. α_0 is written as

$$\nabla_{\alpha_0} J_{\alpha}^{POD} = \mathbf{\Psi}^{\mathbf{T}} \mathbf{B}^{-1} \left(\bar{y} + \Psi \alpha_0 - y^b \right)$$

$$+ \sum_{k=0}^{n} \left(\mathbf{M}_{\mathbf{1}}^{\mathbf{POD}} \right)^{\mathbf{T}} \ldots \left(\mathbf{M}_{\mathbf{k}}^{\mathbf{POD}} \right)^{\mathbf{T}} \mathbf{\Psi}^{\mathbf{T}} \mathbf{H}_{\mathbf{k}}^{\mathbf{T}} d_k$$

where $\left(\mathbf{M}_{\mathbf{k}}^{\mathbf{POD}} \right)^{\mathbf{T}}$ is the POD reduced-order adjoint model at time step k.

Pseudo - Algorithmic form

1. Initialize *reduced-order adjoint variables* α^* at final time to zero: $\alpha_n^* = 0$
2. For each step $k-1$, adjoint variables α_{k-1}^* are obtained by adding reduced-order adjoint forcing term $\mathbf{\Psi}^{\mathbf{T}}\mathbf{H}_{\mathbf{k}}^{\mathbf{T}}d_k$ to $\alpha_k^*$and performing reduced-order adjoint integration by multiplying result by $\left(\mathbf{M}_{\mathbf{k}}^{\mathbf{POD}}\right)^{\mathbf{T}}$, i.e. $\alpha_{k-1}^* = \left(\mathbf{M}_{\mathbf{k}}^{\mathbf{POD}}\right)^{\mathbf{T}}\left(\alpha_k^* + \mathbf{\Psi}^{\mathbf{T}}\mathbf{H}_{\mathbf{k}}^{\mathbf{T}}d_k\right)$
3. At the end of recurrence, the value of adjoint variable $\alpha_0^* = J_{\alpha_0}^o$ yields the gradient of the observational cost functional
4. Compute

$$\nabla_{\alpha_0} J_{\alpha}^{POD,b} = \mathbf{\Psi}^{\mathbf{T}}\mathbf{B}^{-1}\left(\bar{y} + \Psi\alpha_0 - y^b\right)$$

obtaining

$$\nabla_{\alpha_0} J_{\alpha}^{POD} = \nabla_{\alpha_0} J_{\alpha}^{POD,b} + \nabla_{\alpha_0} J_{\alpha}^{POD,o}.$$

Trust region POD optimal control approach

- The Trust - Region algorithm hooks direction of descent and step-size simultaneously. It approximate a certain region, the trust region (a sphere in $\mathbb{R}^n$ of the objective function with a quadratic model function

$$m_k(p) = f_k + \nabla f_k^{\mathbf{T}} + \frac{1}{2} p^{\mathbf{T}} \mathbf{B}_k p, \text{ where}$$

$f_k = f(x_k),\ \nabla f_k = \nabla f(x_k)$ and $\mathbf{B}_k$ is an approximation to the Hessian

- We seek a solution of

$$\min\ m_k(p) = f_k + \nabla f_k^{\mathbf{T}} + \frac{1}{2} p^{\mathbf{T}} \mathbf{B}_k p$$
$$\text{s.t } \|p\| \leq \delta_k,$$

where $\delta_k > 0$ is the trust-region radius.

Trust region POD optimal control approach

- The trust-region radius δ_k at each iteration is determined by analyzing the following ratio

$$\rho_k = \frac{f(x_k) - f(x_k + p_k)}{m_k(0) - m_k(p_k)}.$$

- If $\rho_k < 0$, the new objective value is greater than the current value so that the step must be rejected.
- If ρ_k is close to 1, there is good agreement between the approximate model m_k and the object function f_k over this step, so it is safe to expand the trust region radius for the next iteration
- If ρ_k is positive but not close to 1, we do not alter the trust region radius, but if it is close to zero or negative, we shrink the trust region radius.

Trust region POD 4D-VAR algorithm I

Let $0 < \eta_1 < \eta_2 < 1$, $0 < \gamma_1 < \gamma_2 < 1 \leq \gamma_3$ and $y_0^{(0)}$, δ_0 be given, set $k = 0$

1. Compute snapshot set $\mathcal{Y}_k^{SNAP}$ based on initial condition $y_0^{(k)}$
2. Compute the POD basis $\Psi^{(k)}$ and build up the corresponding POD based control model based on the initial condition $\alpha_0^{(0)} = \left\langle y_0^{(0)} - \bar{y}, \Psi^{(0)} \right\rangle$
3. Compute the minimizer s^k of

$$\min\ m_k\left(\alpha_0^{(k)} + s\right) = J_\alpha^{POD}\left(\alpha_0^{(k)} + s\right)$$

$$\text{subject to } \|s\| \leq \delta_k$$

Trust region POD 4D-VAR algorithm II

4. Compute the new $J\left(\bar{y} + \Psi^{(k-1)}\left(\alpha_0^{(k)} + s_k\right)\right)$ of the full model and

$$\rho_k = \frac{J\left(\bar{y} + \Psi^{(k-1)}\alpha_0^{(k)}\right) - J\left(\bar{y} + \Psi^{(k-1)}\left(\alpha_0^{(k)} + s_k\right)\right)}{m_k\left(\alpha_0^{(k)}\right) - m_k\left(\alpha_0^{(k)} + s_k\right)}$$

5. Update the trust-region radius:
   - If $\rho_k \geq \eta_2$: implement outer projection $y_0^{(k+1)} = \bar{y} + \Psi^{(k-1)}\left(\alpha_0^{(k)} + s_k\right)$ and increase trust-region radius $\delta_{k+1} = \gamma_3\delta_k$ and GOTO 1
   - If $\eta_1 < \rho_k < \eta_2$: implement outer iteration $y_0^{(k+1)} = \bar{y} + \Psi^{(k-1)}\left(\alpha_0^{(k)} + s_k\right)$ and decrease trust-region radius $\delta_{k+1} = \gamma_2\delta_k$ and GOTO 1
   - If $\rho_k \leq \eta_1$: set $y_0^{(k+1)} = y_0^{(k)}$ and decrease trust-region radius $\delta_{k+1} = \gamma_1\delta_k$ and GOTO 3

Flow-chart of Dual Weighted TR-POD

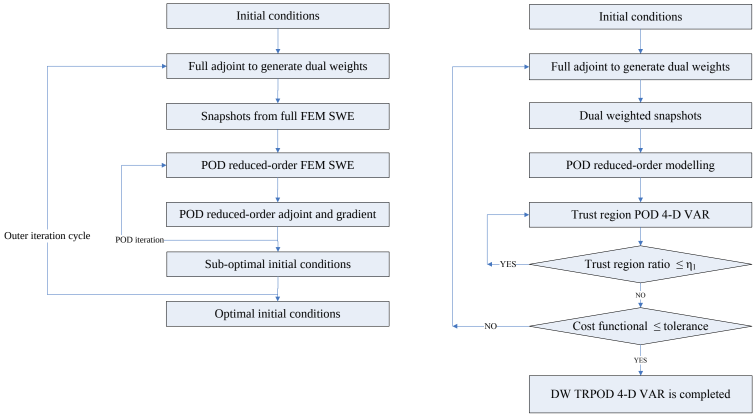

Fig.29 1. adaptive POD reduced order model for dual - weighted snapshots of the full model (left); 2. dual - weighted snapshots and TR-POD adaptivity.

Numerical Results

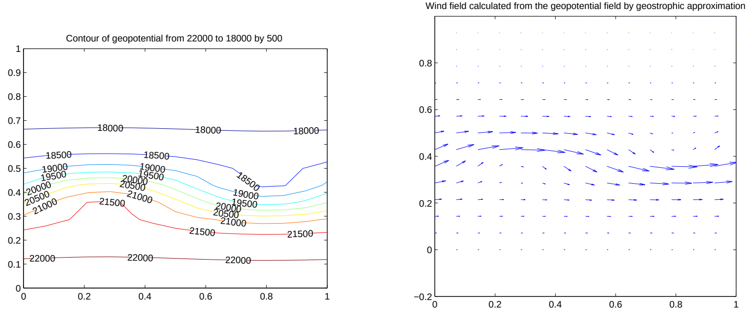

Fig.30 Initial condition:(a) Geopotential field for the Grammeltvedt initial condition. (b) Wind field calculated from the geopotential field by the geostrophic approximation.

Numerical Results

- We employed linear piecewise polynomials on triangular elements in the formulation of Galerkin finite-element shallow-water equations model, in which the global matrix was stored into a compact matrix.
- A time-extrapolated Crank-Nicholson time differencing scheme was applied for integrating in time the system of ordinary differential equations.
- The Galerkin finite-element boundary conditions were treated using the approach suggested by Payne and Irons (1963) and mentioned by Huebner (1975), i.e. modifying the diagonal terms of the global matrix associated withthe nodal variables by multiplying them by a large number, say 10^{16}, while the corresponding term in the right-hand vector is replaced by the specified boundary nodal variable multiplied by the same large factor times the corresponding diagonal term.

Numerical Results

- We applied a 1% uniform random perturbations on the initial conditions in order to provide twin-experiment "observations".
- The data assimilation was carried on a 48 hours window using the $\Delta t = 1800s$ in time and a mesh of 30×24 grid points in space with $\Delta x = \Delta y = 200km$.
- We generated 96 snapshots by integrating the full finite-element shallow-water equations model forward in time, from which we choose 10 POD bases for each of the $u(x,y)$,$v(x,y)$,and $\phi(x,y)$ to capture over 99.9% of the energy.
- The dimension of control variables vector for the reduced-order 4-D Var is $10 \times 3 = 30$.

Numerical Results

- The Polak Ribiere nonlinear conjugate gradient (CG) technique was employed for high-fidelity full model 4-D VAR and all variants of ad-hoc POD 4-D Var, while the steepest-descent strategy was used in the trust-region POD 4-D Var.
- In the ad-hoc POD 4-D Var, the POD bases are re-calculated when the value of the cost function cannot be decreased by more than 10^{-1} for ad-hoc POD 4-D Var and 10^{-2} for ad-hoc DWPOD 4-D Var between the consecutive minimization iterations.
- In the trust-region 4-D Var, the POD bases are re-calculated when the ratio ρ_k is larger than the trust-region parameter η_1 in the process of updating the trust-region radius.

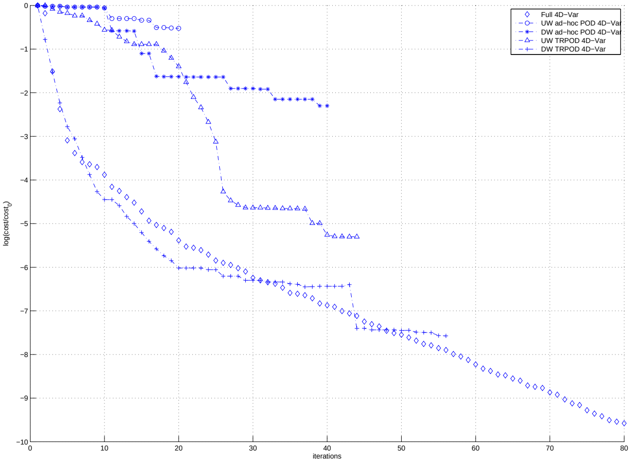

Fig.31 Comparison of the performance of minimization of cost functional in terms of number of iterations for ad-hoc POD 4-D Var, ad-hoc dual weighed POD 4-D Var, trust-region POD 4-D Var, trust-region dual weighed POD 4-D Var and the full model 4-D Var.

- To quantify the performance of the dual weighted trust-region 4-D Var, we use two metrics namely the root mean square error (RMSE) and correlation of the difference between the POD reduced-order simulation and high-fidelity model.

POD 4-D Var	ADPOD	DWAHPOD	TRPOD	DWTRPOD	Full
Iterations	22	42	46	57	80
Outer projections	2	6	10	12	N/A
Error	10^{-1}	10^{-2}	10^{-5}	10^{-8}	10^{-10}
CPU time (s)	15.2	38.7	121.2	142.8	222.6

Table 1 Comparison of iterations, outer projections, RMSE and CPU time for ad-hoc POD 4-D Var, ad-hoc dual weighed POD 4-D Var, trust-region POD 4-D Var, trust-region dual weighed POD 4-D Var and the full model 4-D Var.

- Next image depicts the errors between the retrieved initial geopotential and true initial geopotential applying dual weighted trust-region POD 4-D Var to the 5% uniform random perturbations of the true initial conditions taken as initial guess.

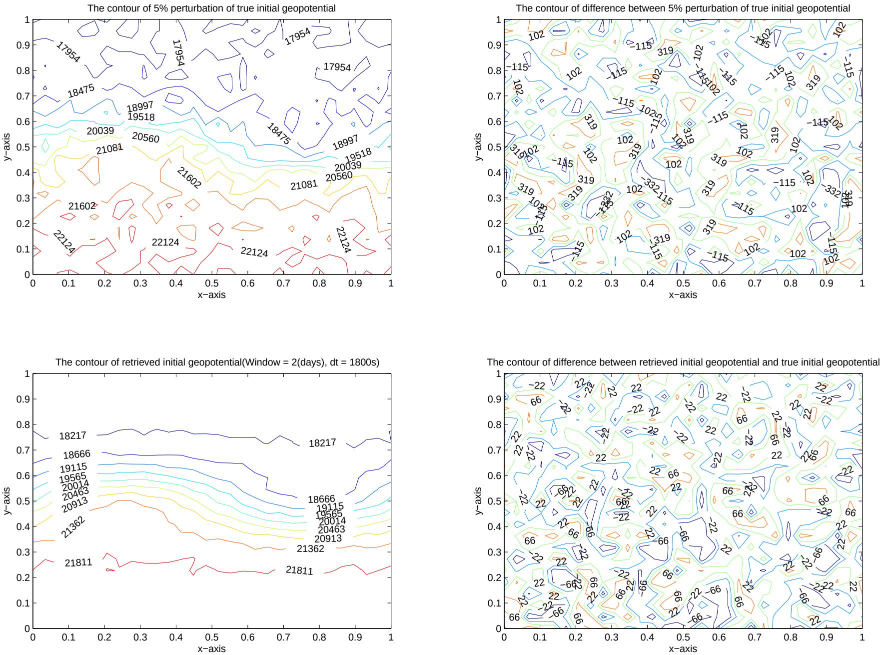
The contour of 5% perturbation of true initial geopotential
The contour of difference between 5% perturbation of true initial geopotential
The contour of retrieved initial geopotential(Window = 2(days), dt = 1800s)
The contour of difference between retrieved initial geopotential and true initial geopotential
y−axis
x−axis

Numerical Results

- The correlation coefficient r used to evaluate quality of the inversion simulation is defined below

$$r_i = \frac{cov_{12}^i}{\sigma_1^i \sigma_2^i},$$

where

$$\sigma_1^i = \sum_{j=1}^{j=N} \left(U_{i,j} - \overline{U}_j\right)^2, \quad \sigma_2 = \sum_{j=1}^{j=N} \left(U_{i,j}^{POD} - \overline{U^{POD}}_j\right)^2, \quad i,j = 1,\dots,n$$

$$cov_{12} = \sum_{j=1}^{j=N} \left(U_{i,j} - \overline{U}_j\right) \left(U_{i,j}^{POD} - \overline{U^{POD}}_j\right), \quad i,j = 1,\dots,n$$

with $\overline{U}_j$ and $\overline{U^{POD}}_j$ are the means over the simulation period $[0, T]$ obtained from the full model and ones obtained by optimal POD reduced-order model at node j, respectively.

Numerical Results

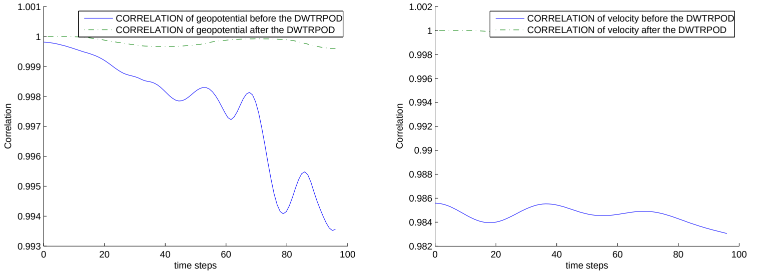

Fig.32 Comparison of the correlation between the full model and the ROM before and after data assimilation applying dual weighted trust-region POD 4-D Var to the 5% uniform random perturbations of the true initial conditions serving as initial guess: geopotential (left), wind field (right).

Numerical Results

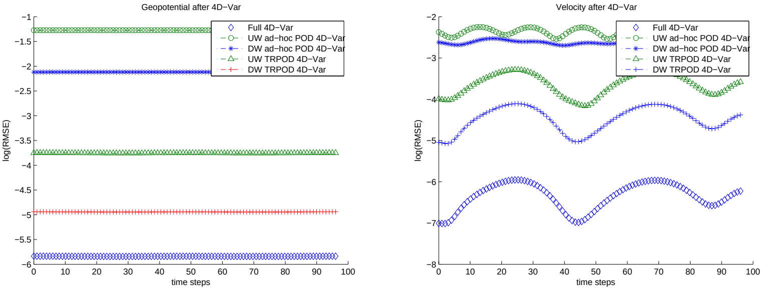

Fig.33 Comparison of the RMSE of between ad-hoc POD 4-D Var, ad-hoc dual weighed POD 4-D Var, trust-region POD 4-D Var, trust-region dual weighed POD 4-D Var and the full model 4-D Var: geopotential (left), wind field (right).

Numerical Results

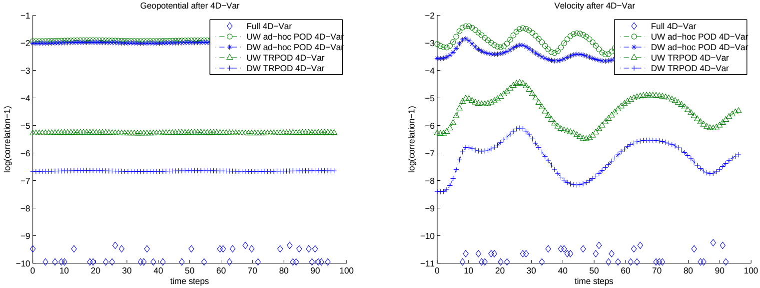

Fig.34 Comparison of correlation between ad-hoc POD 4-D Var, ad-hoc dual weighed POD 4-D Var, trust-region POD 4-D Var, trust-region dual weighed POD 4-D Var and the full model 4-D Var: geopotential (left), wind field (right).

The Global SWE model

- Our intention here is to generalize the efficient state-of-the-art POD implementation from the previous work on finite element SWE on the limited area (FE-SWE) to global finite volume (FV) SWE model with realistic initial conditions, i.e.,
- This methodology combines efficiently the snapshot selection in the presence of data assimilation system by merging dual weighting of snapshots with trust region POD techniques.

The Global SWE model

- The global SWE model was discretized using a semi-lagrangian finite volume scheme, which serves as the dynamical core in the community atmosphere model (CAM), version 3.0, and its operational version implemented at NCAR and NASA is known as finite volume-general circulation model (FV-GCM).
- A two grid combination based on C-grid and D-grid is used for advancing from time step t_n to $t_n + \Delta t$. In the first half of the time step, advective winds (time centered winds on the C-grid: (u^*, v^*)) are updated on the C-grid, and in the other half of the time step, the prognostic variables (h, u, v) are updated on the D-grid.

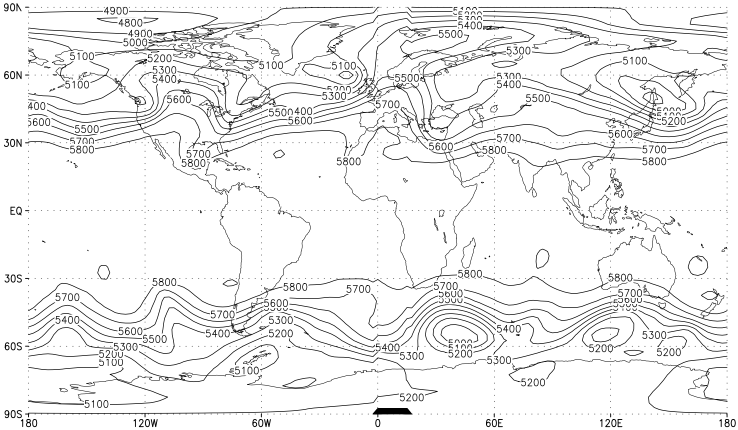

Fig.35 Isopleths of the geopotential height for the reference trajectory. The configuration at the initial time specified from ERA-40 data sets

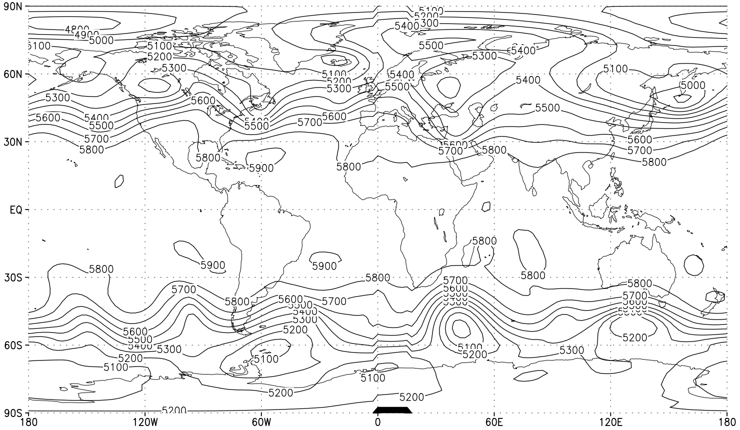

Fig.36 Isopleths of the geopotential height for the reference trajectory. The 18-h forecast of the FV-SWE model

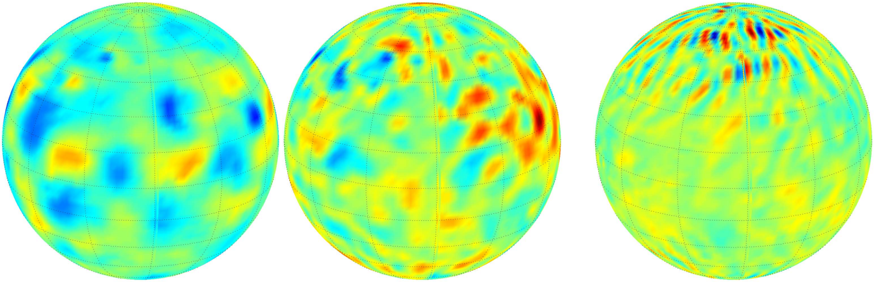

Fig.37 Isopleths of the POD modes of dimension 1, 5 and 10 respectively

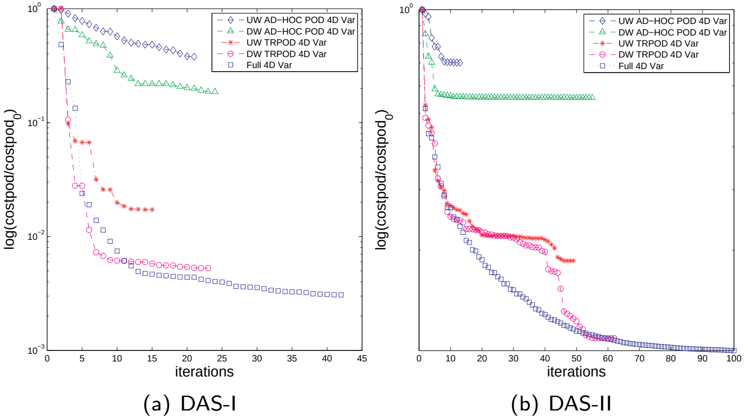

Fig.38 Comparison of the performance of the iterative minimization process of the scaled cost functional for unweighted ad-hoc POD 4-D Var, dual weighted ad-hoc POD 4-D Var, unweighted trust-region POD 4-D Var, dual weighted trust-region 4-D Var, and full model 4-D Var respectively.

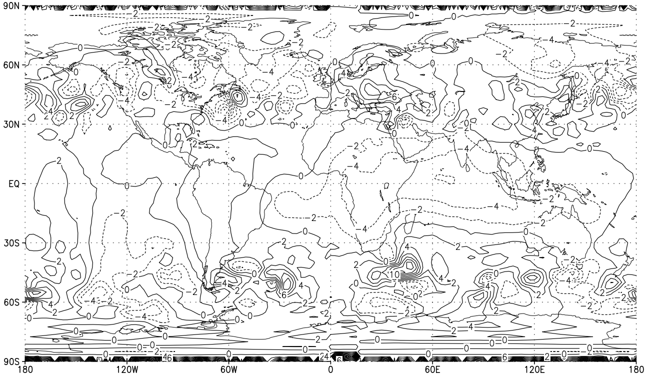

Fig.39 Isopleths(scaled by multiplying 1000) of the geopotential height for the difference between the 18h-forecast using true initial conditions and the one using retrieved initial condition after DWTRPOD 4-D Var - DAS-I

The observations of height field only

- Suppose that only the geopotential field is observed but the observations for the wind field are unavailable (i.e., the number of observations is decreased from $144 \times 72 \times 3 \times 6$ to $144 \times 72 \times 6$).
- We refer to this case by DAS-III(a), in which the initial perturbed field is the same as the one used to start DAS-I.

The observations of height field only

- Suppose that only the geopotential field is observed but the observations for the wind field are unavailable (i.e., the number of observations is decreased from $144 \times 72 \times 3 \times 6$ to $144 \times 72 \times 6$).
- We refer to this case by DAS-III(a), in which the initial perturbed field is the same as the one used to start DAS-I.

The observations of height field only

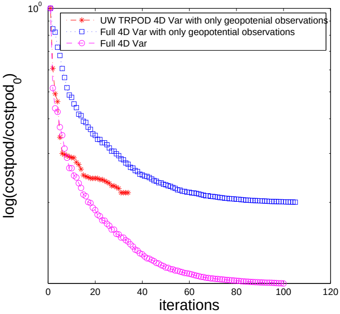

(c) Scaled cost functional

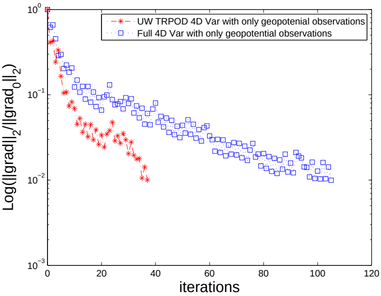

(d) Scaled norm of the gradient

Fig.40 DAS-III(a)(Observations of height field only): Comparison of the performance of the iterative minimization process of the scaled cost functional and the scaled norm of the gradient of the cost functional for unweighted trust-region POD 4-D Var and full 4-D Var.

The observations of height field only

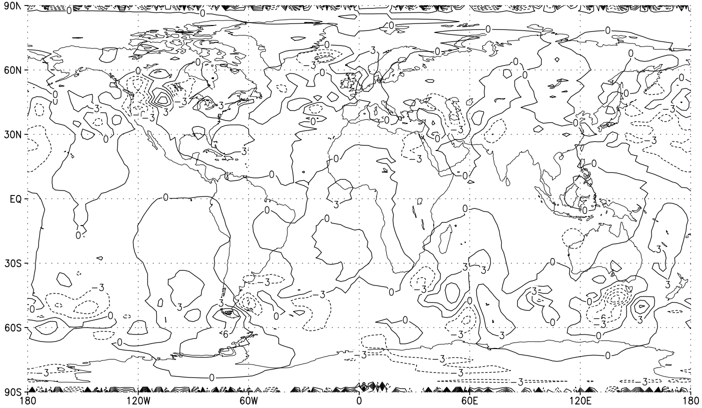

Fig.41 DAS-III(a): Isopleths(scaled by multiplying 1000) of the geopotential height for the difference between the 18h-forecast using true initial conditions and the one using retrieved initial condition after UWTRPOD 4-D Var.

Conclusions

- We compared several variants of POD 4-D Var, namely unweighted ad-hoc POD 4-D Var, dual-weighed ad-hoc POD 4-D Var, unweighted trust-region POD 4-D Var and dual-weighed trust-region POD 4-D Var, respectively.
- We found that the ad-hoc POD 4-D Var version yielded the least reduction of the cost functional compared with the trust-region 4-D VAR . We assume that this result may be attributed to lack of feedbacks from the high-fidelity model.
- The trust-region POD 4-D Var version yielded a sizably better reduction of the cost functional, due to inherent properties of TRPOD allowing local minimizer of the full problem to be attained by minimizing the TRPOD sub-problem. Thus trust-region 4-D Var resulted in global convergence to the high fidelity local minimum starting from any initial iterates.